Wormlike Micelles revisited: A comparison of models for linear rheology

Joseph D. Peterson[1]*, Weizhong Zou[2], Ronald G. Larson[3], Michael E. Cates[4]

October 5, 2023

[1]University of California, Los Angeles, Department of Chemical and Biomolecular Engineering, 420 Westwood Plaza, Los Angeles CA 90024, [2]MIT, Department of Chemical Engineering, 77 Massachusetts Avenue, Cambridge, Massachusetts 02139 [3]University of Michigan, Ann Arbor, Department of Chemical Engineering, 2300 Hayward St., Ann Arbor, MI 48109 [4]Department of Applied Maths and Theoretical Physics, University of Cambridge, Wilberforce Road, Cambridge CB3 0WA, United Kingdom

Abstract

We review a selection of models for wormlike micelles undergoing reptation and chain sequence rearrangement (e.g. reversible scission) and show that many different assumptions and approximations all produce similar predictions for linear rheology. Therefore, the inverse problem of extracting quantitative microscopic information from linear rheology data alone may be ill-posed without additional supporting data to specify the sequence rearrangement pathway. At the same time, qualitative parameter estimates can be obtained equally well from any of the models in question. Our study also provides a careful re-assessment of how to best reconcile artificial chain sequence rearrangement pathways (such as Poisson renewal) with physical processes like reversible scission.

1 Introduction

Wormlike micelles (WLMs) are polymer-like structures that self-assemble from small-molecule surfactants in aqueous solution [1, 2, 3, 4, 5, 6, 7]. In industrial applications, ranging from fast-moving consumer goods to environmental cleanup, WLMs are often preferred to other self-assembled surfactant structures (e.g., spherical micelles or bilayer membranes) because the viscosity and elasticity

*Corresponding author, jdp3@ucla.edu

of a WLM formulation can be adjusted over a wide range by tuning the salt concentration [8, 9, 10, 11]. Familiar applications of WLMs include home and personal care products like shampoos, liquid soaps, and hand sanitizers [12, 13, 14]. In the late 1980s, experimental and theoretical studies of WLM systems expanded considerably, covering both rheology and phase behavior across many surfactant chemistries [15, 16, 17, 18, 19, 20, 21, 22, 23, 24, 25]. Three decades later, WLMs remain a productive research area for the rheology community, and WLMs are often seen as a 'model polymer' platform for studying universal features of nonlinear polymer rheology, viscoelastic flow instabilities, and more [26, 27, 28, 29, 25, 30, 31]. At the same time, WLMs are distinct from traditional covalently bonded polymers in that WLMs can break and reform reversibly, with implications for structure (e.g. length distribution) and rheology.

As pertains to rheology, early conceptual breakthroughs provided valuable mechanistic insights, beginning with the Cates model [15] of reptation with reversible chain scission. The most widely cited conclusions of the Cates model are:

- A polydisperse mixture of WLMs relaxing by reptation will exhibit a single relaxation time τ if the time it takes for a typical WLM to break τ_{B} is much faster than the time it would take a typical WLM to relax by reptation in the absence of reversible scission reactions, $\bar{\tau}_{\mathrm{rep}}$.

- The single relaxation time in question is proportional to the geometric mean of the reptation and breaking times, $\tau \sim [\bar{\tau}_{\mathrm{rep}}\tau_{\mathrm{B}}]^{1/2}$.

However, the full implications of the Cates model are much more nuanced; these two major results alone are not sufficient to support a complete interpretation of linear rheological data for most WLM systems, as one must consider at least four additional layers of complexity. There are: (1) many chain sequence rearrangement pathways besides reversible scission [32, 30, 33]; (2) many relaxation processes besides reptation [34, 35, 36]; (3) many WLM architectures besides flexible linear chains, and (4) many distinct scaling regimes for different relative values of τ_{B} and $\bar{\tau}_{\mathrm{rep}}$ [23, 37, 38]. More challenging still, (5) the same set of nominal assumptions (e.g. reversible scission, no loops or branching) can yield a library of candidate models using different approximations and seemingly unrelated mathematical machinery [15, 16, 34, 39].

In this paper, we will attempt to disentangle some of the complexities associated with (1), (4), and (5) as enumerated above, comparing predictions from models that nominally cover similar systems using different mathematical machinery and/or different representations of the underlying physical processes. Direct comparisons to experimental data are not featured in this discussion, since the models in question have been previously and independently validated in this regard. We will assume the reader has a basic familiarity with Cates' 1987 theory and the physical picture of reptation and reversible scission that it encodes, but no depth of knowledge regarding model details or supporting mathematical machinery.

The complexities of (2) and (3) are out of scope for our present study: we address only linear chain architectures for which the primary relaxation mechanism in the absence of chain sequence rearrangements (such as those caused by reversible scission) is reptation. However, we do acknowledge the practical importance of understanding different relaxation pathways (e.g. contour length fluctuations, constraint release Rouse motion) and different WLM architectures (loops, branches, rods, networks), for which the main conclusions of the present study may not necessarily generalize. A comparison of branched and unbranched WLM rheology will feature in a forthcoming publication [40], and further comparisons must be left to future research.

The rest of this paper is structured as follows. To begin, section 2 reviews the existing space of models, assumptions, and approximations for reptation and chain sequence rearrangement in WLMs. In section 3 we use the 'simplest' model [23] to generate benchmark calculations for direct model/model comparisons to follow in sections 4–6: section 4 compares with different versions of the original 'Poisson Renewal' (PR) model by Granek and Cates [16], section 5, compares with different versions of the 'Pointer method' by Zou and Larson [34], and section 6 compares with a double reptation shuffling model by Peterson and Cates [23]. As a supplementary discussion, section 7 summarizes key ideas in feature-parameter mapping for linear rheology of WLMs, including the effects of intra-tube Rouse modes. The conclusions of sections 4 - 6 are summarized in section 8, where future research directions are discussed.

Overall, we find that the different models of linear WLM rheology that we consider (all intending to describe the same physical problem) are not distinct. By this we mean that if one of the models is suitable to fit some experimental data, an equivalent fit can be obtained from any of the other models (albeit with different parameter inputs). On the basis of this conclusion, we argue that experimentalists and formulation-scientists can be confident in choosing any one of these models to extract usable *qualitative* formulation-property relationships for linear rheology data. The differences between models do however matter, to whatever extent one is interested in using linear rheology data for *quantitative* extraction of kinetic information, such as identifying a specified chain sequence rearrangment pathway (e.g., reversible scission vs. end attack) and the associated rate constants. We find that the rearrangement pathway itself does not leave a clear signature in the linear rheology data, and hence extracting *quantitative* formulation-property relationships from linear rheology *alone* is likely an ill-posed problem. This highlights the need for separate measurements (independent of linear rheology) to corroborate a proposed rearrangement pathway, whenever such quantitative relationships are required.

2 Background

In this section, we will review the basic microscopic processes relevant to WLM rheology, establish a nomenclature for comparing modeling frameworks, and summarize the history and overall landscape of linear constitutive models for WLMs.

2.1 Review of Microscopic Processes

WLMs are sometimes termed 'living polymers', in that their chain-like structures (with contour length vastly exceeding their diameter) resemble polymers, but instead of being formed from a (terminating, generally irreversible) sequence of polymerization reactions, chains of varying molecular weight are formed through a series of (non-terminating, reversible) self-assembly processes [41, 42, 43]. One important self assembly process is reversible scission; the forward reaction sees WLMs spontaneously breaking apart at some random contour position, and the reverse reaction sees WLM ends merging together (cf. Figure 1(b)). At equilibrium, the principle of detailed balance requires that the overall rate of the forward process and the reverse process must be equal. Assuming all WLM ends are equally reactive, the equilibrium number density distribution $n(L)$ as a function of WLM contour length L varies as $n(L) \sim \exp(-L/\bar{L})$, where $\bar{L}$ is the number-average length of a WLM [15].

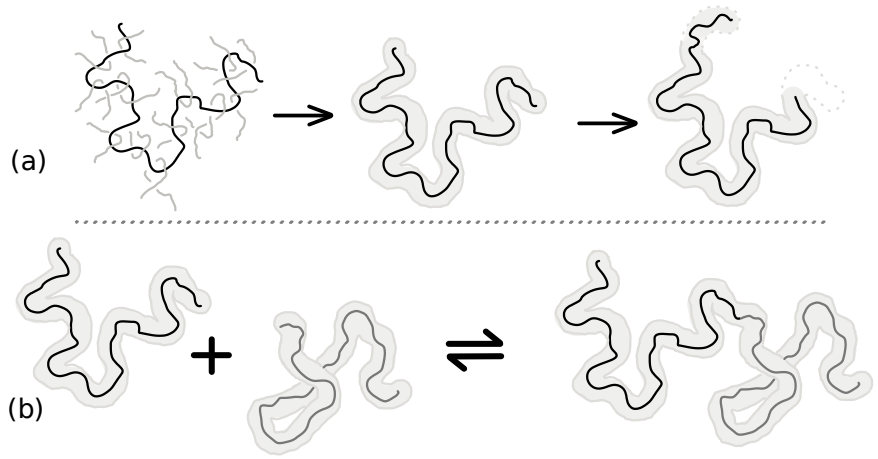

Figure 1: Graphical representations of important microscopic processes for WLMs. (a) Very long WLMs can become entangled such that stress relaxation occurs primarily through reptation. (b) The equilibrium molecular weight distribution of WLMs is determined by sequence rearrangement processes like reversible scission, in which WLMs randomly break apart and recombine.

As the energy needed to break a WLM increases, the typical WLM length grows longer, with an exponential dependence on the scission energy and a power law dependence on the concentration [32, 44, 45]. When the WLMs become very long and are sufficiently concentrated, they

become entangled with one another. For the purpose of this discussion, WLMs are entangled when topological constraints between neighboring WLMs (arising because they cannot pass through one another) strongly restrict the lateral motions of a typical WLM (Figure 1 (a)).

As a WLM diffuses along its own contour, it simultaneously evacuates previously occupied portions of its tube on one side and creates new tube sections on the other. This process of losing the original tube is intrinsically tied to stress relaxation and is known as reptation [46, 47] (see Figure 1(a)). The mechanistic interplay between reversible scission and reptation was first considered by Cates [15], who argued that reversible scission speeds up stress relaxation by converting slow-relaxing interior tube segments to fast-relaxing end segments with every scission event. Note in Figure 1 that when WLMs break or combine, their confining tubes simply merge or divide; there should be no net creation or destruction of tube segments from reversible scission processes alone [39]. This remark will be important in section 4.3.

2.2 Terms and Definitions for Comparisons

Having established the physical context of the problem at hand, there are a number of terms that should be precisely defined before we can begin discussing and comparing different WLM models. Even readers who are deeply familiar with WLM models should read this section carefully, as terms like "rearrangement", "breaking time", and "distinct" will take on specific meanings for the purposes of this paper.

- Rearrangement Mechanisms – In section 2.1, we discussed reversible scission as one possible pathway for chain sequence rearrangement, through which sections of WLM chains are randomly reassigned to different contour positions and different chain lengths. Other chain sequence rearrangements are listed below. In principle, the choice of sequence rearrangement pathway is independent of the choice of mathematical modeling framework (e.g. continuum or stochastic).

  - End attack (also known as "end interchange"): the end of a WLM can insert itself along the length of a neighboring WLM, forming a temporary ternary branch point. The branch point can then break apart, splitting off a fragment from the WLM that was originally attacked.
  - Bond interchange: two WLM can fuse at some point along their contours, forming a temporary quaternary branch point. The branch point can decay back to two linear WLMs, exchanging material in the process.
  - Shuffling: an artificial rearrangement pathway in which WLMs are continuously and randomly reorganized in a uniform way.

  - Poisson renewal: another artificial rearrangement pathway, analogous to shuffling but allowing non-uniform (length-dependent) rates of rearrangement.

- Rearrangement Mathematics – To simulate the rheology of WLM undergoing one of the aforementioned rearrangement processes, there are two basic types of mathematical frameworks that can be used. In principle, either framework can be used to equivalent effect (cf. reversible scission [15, 39]), though in practice the details of each rearrangement processes may naturally favor one approach over the other.

  - Stochastic models: A stochastic model is defined in terms of a Langevin equation (stochastic differential equation) for individual chain dynamics. Stochastic models (such as the Pointer algorithm) are often more flexible, more intuitive, and more easily constructed, but can be computationally expensive compared to continuum models.

  - Continuum models: A continuum model is defined in terms of continuous variables and deterministic equations for ensemble-averaged quantities. Continuum models (such as Poisson renewal and shuffling) are often difficult to set up, but they can be computationally efficient compared to stochastic models.

- Breaking time – For a physical rearrangement pathway (e.g. reversible scission or end attack), the "breaking time" τ_{B} is the average time for a WLM of average length to break. For artificial sequence rearrangement pathways (e.g. shuffling or Poisson renewal) the "breaking time" τ_{B} is a measure of the mean rearrangement time for a typical tube segment, and *cannot necessarily be interpreted as a physical breaking time.*

- Additive process – two stress relaxation processes A and B are 'additive' if their contributions to the relaxation modulus are determined independently and added together, i.e. $G(t) = G_A(t) + G_B(t)$.

- Physics vs. fitting – When comparing a data set with a model, the physics of the model determine whether a good fit *exists in principle*, but whether a good fit *can actually be found* is a separate question that also depends on the optimization engine used to search the model's parameter space.

- Rheologically Distinct vs. indistinct models – Given two models, A and B, with supporting parameter sets α and β, model A is indistinct from model B if for every parameter set α there exists a parameter set β (and vice versa) such that A and B yield practically indistinguishable viscoelastic outputs. Where this condition is not met, models A and B are distinct for some portion of their respective parameter spaces.

2.3 History and Landscape of WLM Models

In this section, we will provide a brief summary of the constitutive models that have been developed to interpret the linear rheology of WLMs. Our goal is to place these models in their historical context and discuss the factors that motivated their development. A summary perspective on comparisons between models can be found in Appendix C.

Cates' initial work on reptation with reaction employed a stochastic modeling approach [15]. The model began by choosing a random point on a random chain and then simulating the processes of reptation (1D random walk of a point particle) and reversible scission (changes in the length of 1D line interval) until the section of tube represented by the point particle relaxed (random walker reaches an endpoint of the 1D interval). Simulating this process many times revealed a distribution of tube survival times and a time-dependent overall tube survival probability $\bar{P}(t)$. The stress relaxation modulus $G(t)$, which describes stress relaxation following a small step deformation, can be computed by multiplying the tube survival probability by a shear modulus G_e, such that $G(t) = G_e\bar{P}(t)$.

In principle it is possible to measure experimentally a relaxation modulus $G(t)$, but a more accurate and convenient measurement of the same information comes via the complex modulus $G^*(\omega)$ for small amplitude oscillatory deformations at varying frequency ω. The relaxation modulus $G(t)$ and complex modulus $G^*(\omega)$ are related by the one-sided Fourier transform (OSFT), $G^*(\omega) = i\omega\int_0^\infty e^{i\omega t}G(t)dt$. The real/imaginary parts of $G^*(\omega)$ are termed the storage/loss moduli and describe the elastic/viscous response of the material at varying frequencies. Both $G(t)$ and $G^*(\omega)$ measure the equilibrium (linear) viscoelastic response of a material, so the micelle size distribution is not perturbed from equilibrium by these measurements. Studying not only $G(t)$ but also $G^*(\omega)$ has been a major preoccupation of every WLM modelling effort, at least since the work of Turner and Cates [48]. It is worth noting that for stochastic models, executing an OSFT is an inherently ill-conditioned problem [49].

A direct numerical evaluation of $G^*(\omega)$ for a WLM model was first developed by Granek and Cates [16], who introduced a complicated multi-dimensional integral constitutive relation (continuum model) for the relaxation modulus $G(t)$. However, $G(t)$ was never solved for directly; instead, the authors showed that when an OSFT is applied to *the constitutive relation itself*, the original PDE collapses into a simpler equation for $G^*(\omega)$ that is trivial to evaluate numerically. The fact that continuum models deal with the OSFT problem so easily is a significant advantage of continuum models over stochastic models.

Granek and Cates also extended the basic reptation-only framework to include additional stress relaxation processes, including contour length fluctuations (CLF) and intra-tube Rouse modes. Both relaxation processes were introduced as piecewise continuous elements in a single-WLM

relaxation modulus $G_0(t)$, effectively making them nonseparable from reptation in the original Poisson renewal approach. This simplifies the calculations, but in general the stress relaxation from faster intra-tube Rouse modes can simply be added to the stress arising from entanglements, provided[1] the breaking time τ_B is much longer than the Rouse time of a single entanglement segment τ_e [34, 39, 51, 52]. This means that one can independently choose models for relaxation at the tube scale (reptation, CLF, etc.) and intra-tube scale (flexible, semiflexible, etc.) [34, 53, 54], and the contributions to the complex modulus $G^*(\omega)$ will be additive. We will therefore restrict our focus to modeling tube-scale relaxation processes and, except for a brief discussion in section 7, *our figures will not capture high frequency features such as a local minimum in the loss modulus.* At the same time, high frequency Rouse modes are very important for a complete material characterization [55, 56, 57, 58], and so a general discussion on the interpretation of Rouse modes is provided in section 7.2.

Around the same time as the Poisson renewal model, an alternative continuum modeling approach was put forward by Lequeux [59]. Lequeux framed WLMs as a population of chains differing in length, generalizing the concept of a "population balance equation" from its conventional context of mass balance (describing changes in the size distribution) to produce an additional balance equation on stress. Lequeux suggested that every time self-assembling structures exchange material (e.g. by reversible scission in the case of WLM), both the mass and the stress of the original structures are transferred to a new sector of the WLM size distribution - a process that can be described with mathematical precision through "stress balance" terms appended to an existing differential constitutive equation for stress relaxation in the absence of rearrangement. Models that preserve this basic structure to describe stress relaxation with physical rearrangement processes will here be called "population balance" constitutive equations.

While Lequeux's work is deeply insightful, it suffers from a few problems. First, the mathematical framework is unwieldy compared to the much simpler Poisson renewal model. Second, the model fails to capture Cates' scaling in the fast-breaking limit due to the use of a single mode approximation for reptation in the absence of rearrangement. Presumably for these reasons, the population balance framework for continuum modeling of WLMs was abandoned for almost three decades after its initial introduction.

Since the Poisson renewal model was first published in 1992, the field of polymer rheology has made many significant advances. New relaxation processes and microscopic insights that were first introduced into polymer theory subsequently incorporated into WLM models [34, 60, 61, 39]. The past three decades have also brought significant advances in computational resources, and so stochastic models have become a viable option for fitting and interpreting experimental data

[1]For well-entangled systems of any WLM chemistry, this approximation should hold to the best of the authors' knowledge. However there are other living polymer systems for which it does not hold [50].

even at large scales. In this context, Zou and Larson developed the 'Pointer model' (physics) and an associated 'Pointer algorithm' (fitting procedure) for interpreting experimental data of $G^*(\omega)$ in well-entangled semi-flexible WLMs [34]. To our knowledge, this was the first WLM model with an accompanying fitting algorithm and also the first to distribute a full open-source model implementation.

All of the above models can make predictions for linear rheology, but when generalized to the nonlinear regime (which is not the main topic of this paper) most lead to constitutive equations of integral form (i.e. based on a memory kernel $G(t)$). The approach by Lequeux was different, leading a a *differential* constitutive equation that could in principle be generalized to include nonlinear relaxation processes. The distinction between differential and integral constitutive relations matters in a practical sense; the former is simpler and more widely used for fluid dynamics calculations. This explains the recent re-emergence [39, 62, 23] of the population-balance approach initiated by Lequeux. Note also that the Vasquez-Cook-McKinley (VCM) model of WLM rheology can also be interpreted as a severely coarse grained population balance approach in which micelles take on only two different lengths [63, 64].

Motivated by growing interest in the quantitative nonlinear rheology of WLMs, Peterson and Leal developed a fully coupled nonlinear population balance constitutive equation for WLMs, borrowing a description of nonlinear relaxation processes from an existing model for well entangled polymers [62]. In its first formulation, this model had the same weaknesses (single-mode approximation and computational complexity) as the Lequeux model, but follow-up work by Peterson and Cates provided corrections that restored key scaling exponents and allowed computationally tractable methods of solution [39, 23]. A new set of continuum models for the linear rheology of WLMs emerged as a part of this larger effort, including (1) a full-chain (i.e. with resolution of tube segments in each chain) population balance model for reversible scission[2] and (2) a simplified approximation of the population balance approach, called 'shuffling' [39, 23]. The relationship between shuffling and reversible scission is discussed in Appendix A.

Besides the models outlined above, there are several others worth noting, but that will not feature in the comparisons to follow. We will not include the Lequeux model, nor will we include any model (such as VCM) that employs a single-mode approximation of reptation [62, 63], as the limitations of a single-mode approxmiation are already well known. Similarly, slip-link models provide an excellent description of CLF [65, 66, 61], but here we will focus on highly entangled systems where CLF is subdominant to reptation, in which case slip-link models become computationally prohibitive. Indeed slip-link models for WLM have only considered a maximum of $\bar{Z} = 9$ entanglements per WLM in studies thus far [61, 67]. Finally, we exclude nonlinear rheology mod-

[2]Considering reptation and reversible scission only, the original Cates model [15], the Pointer model[34], and the full-chain population balance model [39] are all different ways of modeling the exact same underlying processes.

els that build upon a fast-breaking approximation, since these models do not attempt to capture details of linear rheology outside the limit where reversible scission is much faster than reptation (for which linear rheology is essentially Maxwellian [68, 39, 69]). Instead, we will focus on linear rheology models featuring a full-chain description of reptation in flexible WLMs, and we allow for diverse means of describing WLM sequence rearrangements (i.e. not limited to reversible scission). Specifically, our study will compare predictions of the Poisson renewal model, the Pointer model, and the shuffling model.

In each of these modeling frameworks, one can make rheological predictions for linear WLMs undergoing reptation with some kind of underlying pathway for WLMs to rearrange their material. Likewise, all of these frameworks have been independently shown to match well to experimental data on linear rheology, including effects of multiple relaxation times. If the models are distinct, then whichever model provides the *best* fit to a given set of data likely provides the most reliable interpretation of the underlying physical processes. However, if the models are not distinct then an equivalent fit can be obtained from any choice of model, each implying a different description of the underlying physical processes. Where multiple models appear equally valid, fitting parameters can only provide qualitative (not quantitative) microscopic insights regardless of the goodness of fit until the underlying rearrangement pathway can be independently ascertained.

A central question that we aim to address is therefore given as follows: when fitting to linear rheology data, absent any other supporting information, are the model predictions distinct so that a good fit to data validates the model and fitting parameters, or indistinct, so that each model can give an equivalent fit, using different model-dependent parameters to achieve that fit?

The organization of our study is as follows. In section 3, we use the shuffling model to generate a set of benchmark calculations against which calculations using other models can be compared. In section 4 we review the original Poisson renewal model and compare its predictions to the benchmark calculations. Newly identified problems with the Poisson renewal model (and possible corrections) are discussed in sections 4.3 and 4.4. In section 5, several versions of the Pointer model (single reptation, double reptation, end attack) are compared with the benchmark calculations, using the Pointer algorithm to handle the parameter search. In section 6 we compare the shuffling model with and without constraint release by double reptation to determine whether these two versions of the model are distinct. Finally, section 7.2 discusses the importance of high frequency Rouse modes for interpreting experimental data.

Across all of these comparisons, we find that *none of the models are distinct* for the practical purpose of providing a fit to experimental data if those data are dominated by low and moderate-frequency reptation and breakage/rejoining effects, excluding higher-frequency dynamics such as CLF, Rouse relaxation, and bending modes. We also find that stochastic models tend to struggle with fitting $G^*(\omega)$ at high frequencies due to the ill-conditioned OSFT problem.

3 Shuffling Model Predictions

In this section, we will review the shuffling model developed by Peterson and Cates [39, 23] (subsection 3.1) and then generate a set of benchmark results to facilitate our search for distinct model predictions (subsection 3.2). We choose the shuffling model as our benchmark because it is the simplest model to explain and the fastest to compute. Section 3.1 is primarily intended as a review for readers not yet familiar with reptation models and the general Cates theory for reptation with reversible scission. Other readers can continue to section 3.2.

3.1 Basic Cates theory via reptation and shuffling: a review

The shuffling model begins from an equilibrium distribution of WLM lengths, $n(L) \sim \exp(-L/\bar{L})$, where $n(L)$ gives the number density of WLMs with contour length L in solution and $\bar{L}$ is the number-average length [15]. As with all of the models considered here, we neglect loops and branches, and assume that the typical WLM is long enough to neglect minimum size constraints (i.e., much longer than the diameter). As per classical reptation theory, when WLMs are very long they become entangled, and constraints on lateral (as opposed to curvilinear) movement are interpreted as a confining tube-like potential. Polymer stress is tied to the orientation of these tube segments, which are treated as fixed topological constraints: the only way for stress to relax is for a polymer to diffuse along its own contour, or 'reptate', to escape its confining tube and establish a new tube configuration that is stress free.

To frame the above statements more precisely, we define a function $P(t, s, L)$ to keep track of the mean 'tube survival probability' for a tube segment on a WLM of length L, initially at contour position $s \in [0, L]$, at time t. The mean tube survival probability $\bar{P}(t)$ is averaged across all WLM lengths and all contour positions to describe the overall fraction of initial tube segments that have been able to relax. The WLM stress decays in proportion to the surviving tube segments, $G(t) = G_e\bar{P}(t)$, where the constant of proportionality is a shear modulus G_e. WLM ends are always taken to be stress free, $P(t, s = 0, L, L) = 0$, and at $t = 0$ the system is initialized with all the original tube segments in place, $P(t = 0, s, L) = 1$. Finally, in the absence of reversible scission or any such sequence rearrangements, reptation theory describes tube survival via 1D diffusion of a flexible polymer along its own contour with a mobility that scales inversely with the polymer length, $M = M_0/L$ with $M_0 = \bar{L}^3/\pi^2\bar{\tau}_{\text{rep}}$ or equivalently[3] $\bar{\tau}_{\text{rep}} = \bar{L}^3/\pi^2 M_0$.

[3]Sometimes the expression given for the reptation time $\bar{\tau}_{\text{rep}}$ drops the coefficient of π^2, as was done in the original Poisson renewal model and shuffling model, but the Pointer model includes it. Therefore, when we report calculations from the Poisson renewal model and the shuffling model, the numerical values of ζ are larger (by a factor of π^2) than they would be if those models' original definition of $\bar{\tau}_{\text{rep}}$ were considered.

All of the above ideas can be expressed in the form of a PDE:

$$\frac{\partial}{\partial t}P(t,s,L) = \frac{1}{L}M_0\frac{\partial^2}{\partial s^2}P(t,s,L) \tag{1}$$

$$P(t,s=0,L,L) = 0 \tag{2}$$

$$P(t=0,s,L) = 1 \tag{3}$$

Any model with the same WLM size distribution $n(L)$ and the same basic description of reptation (whether stochastic or continuous) will ultimately yield an identical result when sequence rearrangements are present but infinitely slow, $\tau_{\mathrm{B}}/\bar{\tau}_{\mathrm{rep}} \to \infty$.

Where sequence rearrangements cannot be ignored, describing processes like reversible scission or end attack with mathematical precision is possible but complicated [39]. Fortunately, a 'shuffling' rearrangement is simple to describe and captures many of the same ideas. We refer the reader to Appendix A for further discussion on the relationship between reversible scission and the shuffling model.

The shuffling approximation of WLM rearrangements supposes that segments are uniformly, randomly, and continuously reshuffled with a characteristic timescale τ_{B}. In PDE form, this is achieved by appending a shuffling term to the end of equation 1:

$$\frac{\partial}{\partial t}P(t,s,L) = \frac{1}{L}M_0\frac{\partial^2}{\partial s^2}P(t,s,L) + \frac{1}{\tau_{\mathrm{B}}}(\bar{P}(t) - P(t,s,L)) \tag{4}$$

$$\bar{P}(t) = \frac{\int_0^\infty dLn(L)\int_0^L dsP(t,s,L)}{\int_0^\infty dLn(L)L} \tag{5}$$

$$P(t,s=0,L,L) = 0 \tag{6}$$

$$P(t=0,s,L) = 1 \tag{7}$$

Equation 4 will be called the "shuffling model", and the use of a shuffling term, $\bar{P} - P$, will be called the "shuffling approximation" wherever it is used as an approximation of a different defined sequence rearrangement pathway. The relationship between the shuffling approximation and true reversible scission is discussed in Appendix A.

The complex modulus for the shufflnig model is given by:

$$\frac{G^*(\omega)}{G_e} = i\omega\left[\frac{\langle\eta_0\rangle}{1-\langle\eta_0\rangle/\tau_{\mathrm{B}}}\right] \tag{8}$$

$$\langle\eta_0\rangle = \int_0^\infty dze^{-z}z\left[\sum_{p,\mathrm{odd}}^{\infty}\frac{1}{p^2}[1/\tau_{\mathrm{B}} + i\omega + p^2/\bar{\tau}_{\mathrm{rep}}/z^3]^{-1}\right] \tag{9}$$

$$z = L/\bar{L} \tag{10}$$

The notation in equations 8 and 9 is chosen to emphasize commonality with the Poisson renewal model equations as originally published (cf. equations 14 and 15).

As we will discuss in section 4.4, describing the 'shuffling time' as a 'breaking time' is a convenience, used here to streamline the nomenclature of this paper. In reality, reversible scission and shuffling are different processes, and intuitions on the relationship between the two can be misleading. The derivation of equation 8 from equation 4 can be found in Ref. [39] and will not be reproduced here.

For a maximally efficient numerical implementation of the shuffling model, the infinite sum in equation 9 can be collapsed to a closed-form, leaving a single 1D quadrature as the limiting calculation:

$$\langle \eta_0 \rangle = \bar{\tau}_{\text{rep}} \int_0^\infty dz e^{-z} \frac{z}{A} \left[1 + \frac{2}{z\sqrt{A}} \tanh\left(\frac{z\sqrt{A}}{2} \right) \right] \tag{11}$$

$$A = z(i\omega\bar{\tau}_{\text{rep}} + \bar{\tau}_{\text{rep}}/\tau_{\text{B}}) \tag{12}$$

3.2 Benchmark calculations

The shuffling model has three fittable material parameters: a shear modulus G_e; a reptation time $\bar{\tau}_{\text{rep}}$, and a breaking time τ_{B}. If the complex modulus is scaled by the shear modulus G_e and the imposed frequency is scaled by the reptation time $\bar{\tau}_{\text{rep}}$, then the only remaining parameter (and the one that determines the shape of $G'(\omega)$ and $G''(\omega)$) is the ratio of the breaking time and the reptation time, $\zeta = \tau_{\text{B}}/\bar{\tau}_{\text{rep}}$. This same argument applies to the Poisson renewal model and Pointer model as well.

In Figure 2, we compare predictions for the loss modulus $G''(\omega) = \text{Im}(G^*(\omega))$ as a function of frequency for ζ ranging from very small, $\zeta = 10^{-3}$, to very large, $\zeta = 10^5$. For very large values, $\zeta > 10^3$, predictions become independent of ζ; the rearrangements are so slow that most chains are able to relax by reptation before they experience a rearrangement. For very small values, $\zeta \ll 1$, the frequency response for $\omega\tau_{\text{B}} < 1$ approximates a single-mode Maxwell material. At higher frequencies, $\omega\tau_{\text{B}} \gg 1$, relaxation processes are fast enough to proceed unchanged by WLM rearrangements and all curves collapse. Here, we remind the reader that intra-tube Rouse modes are considered a separate, additive, contribution to the stress; those terms are omitted here, and so figure 2 does not show a local minimum in $G''(\omega)$ (see discussion in section 2 and 7).

For very large values of ζ, WLM rearrangements are negligible and there will be no distinction between any of the models we consider (apart from the distinction of single vs double reptation, cf. section 6). Likewise, for very small values of ζ, all of these models have previously been shown to recover single-mode Maxwell rheology at frequencies $\omega\tau_{\text{B}} < 1$. Therefore, to search for distinctive

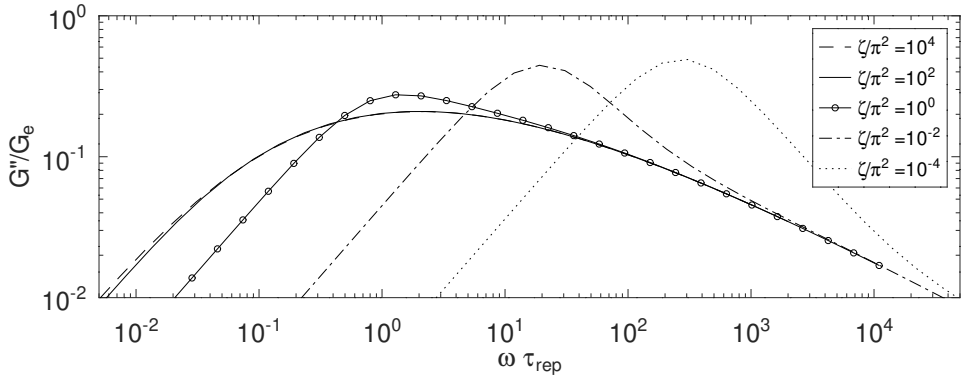

Figure 2: Comparing the loss modulus G''/G_e as a function of frequency $\omega\bar{\tau}_{\text{rep}}$ for varying values of $\zeta = \tau_{\text{B}}/\bar{\tau}_{\text{rep}}$. For very small values of ζ, the peak in the loss modulus shifts towards higher frequencies, and for very large values of ζ (or very large frequencies, $\omega\bar{\tau}_{\text{rep}} > 1/\zeta$) the loss modulus collapses to a single curve. Note that these loss moduli exclude a separable contribution from the intra-tube Rouse modes (discussed in section 2 and section 7) and therefore do not show an upturn at high frequencies.

features we will focus on predictions at intermediate values of $\zeta \sim \mathcal{O}(1)$. For simplicity, we report results for just two values; (1) $\zeta = \pi^2$ gives a system that is transitional between fast breaking $\zeta \ll 1$ and slow breaking scenarios, and (2) $\zeta = 0.01\pi^2$ gives a system that is fast breaking but still shows a clear break from ideal Maxwell behavior. In the text, these values of ζ will be rounded to $\zeta = 10$ and $\zeta = 0.1$. Here and elsewhere[4], the complex modulus will be rescaled by the zero shear steady state recoverable compliance modulus $J_e^0 = \lim_{\omega\to 0} \dfrac{G'(\omega)}{G''(\omega)^2}$ and the frequencies will be scaled by the terminal relaxation time $\tau_0 = \lim_{\omega\to 0} \dfrac{G'(\omega)}{G''(\omega)\omega}$. Scaling this way guarantees agreement in the limit $\omega \to 0$, so we only need to compare the high frequency response at different values of ζ to test whether two models are distinct, in the sense defined in section 2.

Benchmark calculations for the shuffling model with $\zeta = 10$ and $\zeta = 0.1$, scaled to collapse in the zero frequency limit as described in the preceding paragraph, are reported in Figure 3. The main focus of this paper is to see whether different models (e.g. Pointer, Poisson renewal, etc.) can reproduce similar curves using (potentially) different values of ζ.

We have been careful to present our calculations in terms of a rescaled frequency-dependent complex modulus $G^*(\omega)$ rather than a parametric Cole-Cole plot of loss modulus vs storage modulus. This is because the Cole-Cole plot loses frequency information and cannot provide a complete test of distinctiveness; in principle, predictions of $G^*(\omega)$ that are strikingly different could appear identical under a Cole-Cole representation.

[4]Comparisons featuring the Pointer model in section 5 will rescale by J_e^0 and τ_0 as defined by the benchmark (shuffling) calculations. This breaks any guarantee of agreement in the zero frequency limit but preserves the "best fit" identified by the Pointer model's fitting algorithm.

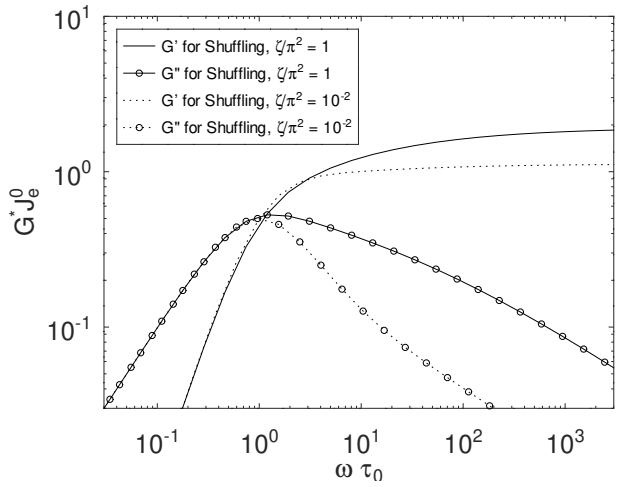

Figure 3: Benchmark calculations for the loss modulus $G''(\omega)$ and storage modulus $G'(\omega)$ for $\zeta = 10$ and $\zeta = 0.1$. All curves have been shifted to ensure agreement in the low frequency range.

4 Poisson Renewal Model

The shuffling model, as defined in equation 4, assumes a constant value of τ_{B}. In this section, we allow the rate of rearrangement to vary across different sectors of the length distribution and explore the resulting implications. For bulk rheology, we find that a length-dependent $\tau_{\mathrm{B}}(L)$ recovers the bulk rheology equations of the Poisson renewal equation (subsection 4.1). We compare the bulk rheology predictions of the Poisson renewal model against the benchmark calculations (subsection 4.2) and then provide physical and mathematical arguments in favor of a constant value of τ_{B} (subsections 4.4 and 4.3).

Readers who are only interested in a practical comparison of Poisson renewal and shuffling calculations can proceed directly to subsection 4.2, skipping subsections 4.1, 4.4, and 4.3. Readers who are interested in developing a deeper understanding of the subtle distinctions between models should find the rest useful.

4.1 Review of the Poisson renewal model

In this section, we will consider a generalization of the shuffling model for which the breaking time varies with WLM length:

$$\frac{\partial}{\partial t}P(t,s,L) = \frac{1}{L}M_0\frac{\partial^2}{\partial s^2}P(t,s,L) + \frac{1}{\tau_{\mathrm{B}}(L)}(\bar{P}(t) - P(t,s,L)) \tag{13}$$

Integrating these equations (following the derivation in Appendix B of Peterson and Cates [39]) we obtain the constitutive equation from the Poisson renewal model:

[16]:

$$\frac{G^*(\omega)}{G_e} = i\omega\left[\frac{\langle\eta_0\rangle}{1-\langle\eta_0/\tau_{\mathrm{B}}\rangle}\right] \tag{14}$$

$$\langle\eta_0/\tau_{\mathrm{B}}\rangle = \int_0^\infty dz e^{-z} z \frac{1}{\tau_{\mathrm{B}}(z)}\left[\sum_{p,\mathrm{odd}}^{\infty}\frac{1}{p^2}[1/\tau_{\mathrm{B}}(z) + i\omega + p^2/\bar{\tau}_{\mathrm{rep}}/z^3]^{-1}\right] \tag{15}$$

$$z = L/\bar{L} \tag{16}$$

A comparison of the rearrangement mechanisms for shuffling and Poisson renewal (as described in the original publication [16]) is interesting but beyond the scope of this section. Some details are give in Appendix B.

To motivate the need for a length-dependent $\tau_{\mathrm{B}}(L)$, the Poisson renewal model noted that longer chains rearrange (i.e. break) more quickly than short chains. For reversible scission rearrangements, the Poisson renewal model uses:

$$\frac{\tau_{\mathrm{B}}}{\tau_{\mathrm{B0}}} = \frac{3.3}{2 + L/\bar{L}} \tag{17}$$

and for WLMs that rearrange by the 'end attack' pathway, the Poisson renewal model uses:

$$\frac{\tau_{\mathrm{B}}}{\tau_{\mathrm{B0}}} = \frac{4.0}{1 + L/\bar{L}} \tag{18}$$

The numerators of these expressions were determined via a fitting process, comparing with predictions from a stochastic model of reversible scission and end attack rearrangement pathways. From the denominators, we see that the breaking time is constant for short chains and inversely proportional to length for very long WLMs. Here, τ_{B} is therefore the *overall* "renewal time" for a chain to react, whether by scission or recombination, but we are calling it a "breaking time" to maintain a common nomenclature for model/model comparisons. For Poisson renewal, we define $\zeta = \tau_{\mathrm{B0}}/\bar{\tau}_{\mathrm{rep}}$, where τ_{B0} is intended to capture the true characteristic breaking time for reversible scission.

4.2 Comparison between benchmark and Poisson renewal

For the Poisson renewal model with reversible scission (equations 17 and 4), we find that the benchmark predictions of the shuffling model for $\zeta = 10$ and $\zeta = 0.1$ can be reproduced, respectively, by using instead $\zeta = 20$ and $\zeta = 0.15$ in the Poisson renewal model. These results are shown in Figure 4.

For the Poisson renewal model with end attack (equations 18 and 4), we find that the benchmark predictions of the shuffling model for $\zeta = 10$ and $\zeta = 0.1$ can be reproduced, respectively, using

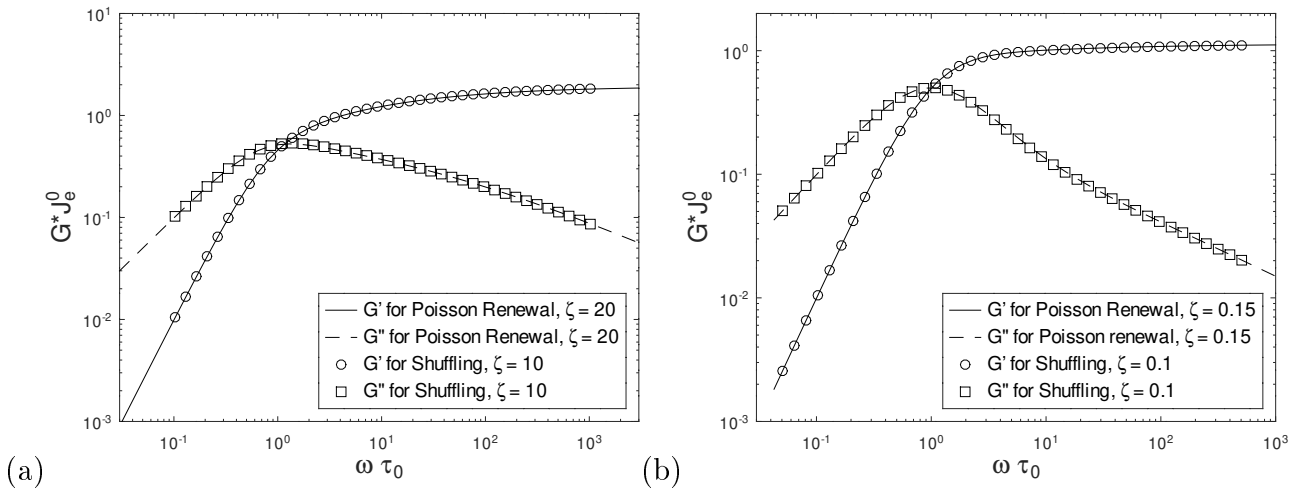

Figure 4: Comparing predictions of the Poisson renewal model with reversible scission (equations 17 and 4) against the benchmark calculations of the shuffling model with (a) $\zeta = 10$ and (b) $\zeta = 0.1$, cf. Figure 3. There is no obvious distinction apart from the differing fitted value of (a) $\zeta = \tau_{\mathrm{B}0}/\bar{\tau}_{\mathrm{rep}} = 20$ and (b) $\zeta = \tau_{\mathrm{B}0}/\bar{\tau}_{\mathrm{rep}} = 0.15$ in the Poisson renewal model.

$\zeta = 15$ and $\zeta = 0.1$ in the Poisson renewal model. These results are shown in Figure 5.

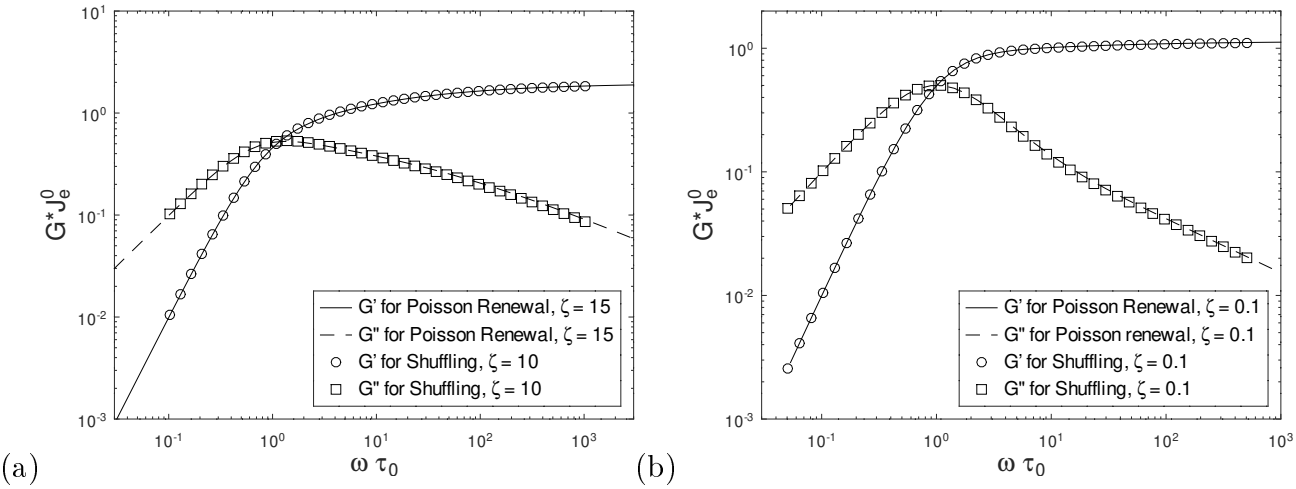

Figure 5: Comparing predictions of the Poisson renewal model with end attack (equations 18 and 4) against the benchmark calculations of the shuffling model with (a) $\zeta = 10$ and (b) $\zeta = 0.1$, cf. Figure 3.

The main difference between Poisson renewal and shuffling appears to be the choice of parameters needed to fit a particular data set and not the range of data sets suitable for fitting. Thus, the inverse problem of extracting kinetic parameters from conventional linear rheology data *alone* is likely ill-posed without additional information to inform the choice of a sequence rearrangement pathway. Further discussion on this subject is given in section 7.2.

Given that different functional forms of τ_{B} can lead to the same quality of fit, it is important to remember that one major purpose of fitting to experimental data is to extract model parameters

(e.g. G_e, τ_{B} or τ_{B0}, $\bar{\tau}_{\mathrm{rep}}$), and these model parameters should describe real physical processes even where the Poisson renewal or shuffling models themselves do not. If the fitted parameters do not consistently map to the physical value of τ_{B} for a given system, this should be regarded as a scientific shortcoming. For example, if different models (all providing very good fits) give incompatible predictions for τ_{B}, then the quantitative value of a true WLM breaking time cannot be determined from rheology data alone.

Where there is independent verification of a specific kinetic pathway for sequence rearrangements (e.g., reversible scission or end attack), can we determine what form of $\tau_{\mathrm{B}}(L)$ (exemplified by equations 17, 18) will be best for mapping experimental spectra onto the mechanistically correct kinetic parameters? In subsections 4.3 and 4.4, we identify potential problems in the original Poisson renewal construction, arguing in favor of a length-independent τ_{B} for shuffling approximations of reversible scission and end-attack rearrangements.

4.3 Concerns regarding conservation relationships

In the Cates framework for WLM rheology, rearrangements do not directly lead to stress relaxation. Instead, they indirectly facilitate stress relaxation by turning slow-relaxing interior tube segments into fast-relaxing end segments. In other words, rearrangements do not create or destroy tube segments but only move them from one WLM chain to another, changing their distance from the nearest chain end in the process. Surprisingly, an unintended consequence of a length-dependent $\tau_{\mathrm{B}}(L)$ is that shuffling rearrangements no longer conserve tube segments. Averaging equation 13 over all chain lengths and all contour positions yields:

$$\frac{\partial}{\partial t}\bar{P} = \left[-2M_0\langle \frac{1}{L}\frac{\partial P}{\partial s}\bigg|_{s=0} \rangle \right] + \left[\langle \tau_{\mathrm{B}}^{-1} \rangle \bar{P} - \langle \tau_{\mathrm{B}}^{-1} P \rangle \right] \tag{19}$$

where

$$\langle X \rangle = \frac{\int_0^\infty n(L)dL \int_0^L X(s,L)\, ds}{\int_0^\infty n(L)dL \int_0^L ds}$$

The first term on the right hand side of equation 19 describes relaxation by reptation, and the second block of terms describes the overall creation/destruction of tube segments happening directly via shuffling. If the shuffling process conserved tube segments, the second block would be identically zero at all times, but this is only guaranteed to hold if τ_{B} is independent of length[5].

To guarantee conservation of surviving tube segments in a shuffling model with length-dependent rates of rearrangement, the mean tube survival probability in a "renewed" chain should not be the

[5]This issue is clearly demonstrated for a shuffling mechanism, but it is also present for the original Poisson renewal rearrangement mechanism. Additional notes on the original description of the Poisson renewal mechanism are given in Appendix B

population-average tube survival probability. Instead, it should be weighted by the rate at which chains of different lengths make themselves available to rearrangement. In other words, we can redefine $\bar{P}$ in equation 13 to be the average tube survival probability of WLMs presently being rearranged.

$$\bar{P}(t) = \frac{\langle P/\tau_{\mathrm{B}} \rangle}{\langle 1/\tau_{\mathrm{B}} \rangle} = \frac{\int_0^\infty n(L)dL \int_0^L dsP(t,L,s)/\tau_{\mathrm{B}}(L)}{\int_0^\infty n(L)dL \int_0^L ds 1/\tau_{\mathrm{B}}(L)} \tag{20}$$

We can call this Poisson renewal with a common pool. Enforcing a common pool for rearrangements is a significant change from the original Poisson renewal formulation, as the bulk rheology is now given by:

$$\frac{G^*(\omega)}{G_e} = i\omega \left[\frac{\langle \eta_0/\tau_{\mathrm{B}} \rangle}{\langle 1/\tau_{\mathrm{B}} \rangle - \langle \eta_0/\tau_{\mathrm{B}}^2 \rangle} \right] \tag{21}$$

$$\langle 1/\tau_{\mathrm{B}} \rangle = \int_0^\infty dz e^{-z} z \frac{1}{\tau_{\mathrm{B}}(z)} \tag{22}$$

For τ_{B} following equation 17, we solve equation 21 and find that the shuffling calculations with $\zeta = 10$ and $\zeta = 0.1$ can be reproduced with $\zeta = 55$ and $\zeta = 0.4$, respectively. Thus the common pool approximation is not distinct from the original Poisson renewal model.

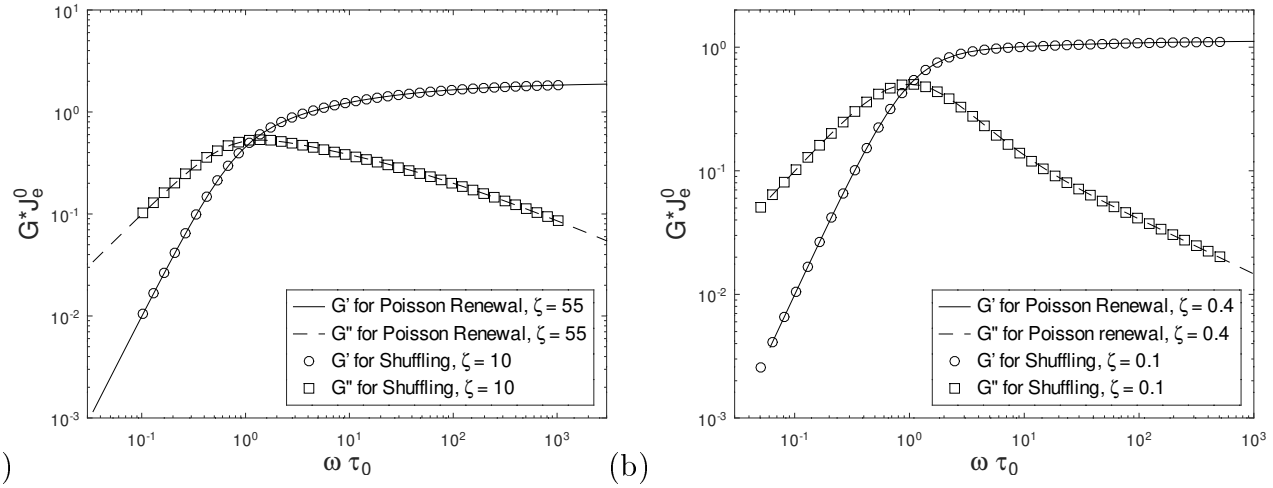

(a) (b)

Figure 6: Comparing predictions of the Poisson renewal common pool model with reversible scission (equations 17, 4 and 20) against the benchmark calculations of the shuffling model with (a) $\zeta = 10$ and (b) $\zeta = 0.1$, cf. Figure 3.

4.4 Detailed balance and the concept of renewal

In Cates' original work on reptation and reaction, it was shown that reversible scission leads to faster stress relaxation because it transforms slow-relaxing interior portions of a WLM into fast-relaxing end portions. This happens every time a WLM breaks, but when two WLMs reattach

there is no resulting stress relaxation. Any approximate sequence rearrangment strategy (e.g. Poisson renewal or shuffling) should attempt to capture the rate at which slow-relaxing interior segments are moved to a WLM end.

In equation 13, WLMs of length L are removed from the population at length L with rate $1/\tau_{\mathrm{B}}(L)$ and replaced at the same rate by chains with the same length and a uniform internal distribution of tube segments with mean tube survival probability $\bar{P}$. For reversible scission, equilibrium reaction kinetics dictate that WLMs of length L are removed from the population at length L at a rate of $2/\tau_{\mathrm{B0}}$ by recombination and a rate of $L/(\bar{L}\tau_{\mathrm{B0}})$ by reversible scission. Therefore, it would seem sensible to formulate a shuffling model with a breaking time that includes both of these processes, cf. equation 17. Unfortunately, this misses a key distinction: chains of length L produced by scission of long chains $L' > L$ are very different from chains of length L produced by recombination of shorter chains $L' + L'' = L$. For recombination events, no new ends are created.

By detailed balance, every time a WLM of length L breaks it must be replaced by a pair of shorter WLMs (in some other, possibly distant part of the system) with lengths $L' < L$ and $L'' = L - L'$ undergoing the reverse process of recombination. In recombination, there is no transfer of interior segments to end segments, and therefore no path for faster stress relaxation in the population of WLMs with length L. For WLMs of length L, faster stress relaxation is only possible when the micelle in question was generated by scission of a longer micelle.

Integrating over all possible breaking events for all WLMs longer than length L seems difficult, but detailed balance provides a solution. At equilibrium, the rate at which WLMs of length L form by scission of longer WLMs must be equal to the rate of the reverse process at which WLMs of length L undergo recombination. For reversible scission (assuming equal reactivity of end segments), the latter is given by $2/\tau_{\mathrm{B0}}$, and is independent of length. Furthermore, since fragments of length L have one relaxed end and one unrelaxed end, the rate at which renewed chain ends are produced for chains of length L must be half of this rate, $1/\tau_{\mathrm{B0}}$. Therefore, we argue that a constant τ_{B} (rather that the L-dependent one used in the original Poisson renewal approach) will provide a better approximation of the essential Cates mechanism, because it gives the true rate at which slow-relaxing interior segments are "renewed", i.e. transformed to fast-relaxing end segments.

For an alternative means of arriving at the same conclusion, Appendix A discusses a set of approximations by which a shuffling model with constant τ_{B} can be derived from the full reversible scission equations.

5 Pointer Algorithm

Similarities between shuffling (which is our benchmark) and Poission renewal may not be too surprising in retrospect, given that the two models have similar equations for bulk rheology. In contrast, the Pointer model has a completely different construction, capturing genuine WLM sequence rearrangements caused by identifiable kinetic schemes like reversible scission and end attack. By comparing against predictions from the Pointer model, we can assess the influence of the shuffling approximation directly.

In its complete form, the Pointer model includes a library of descriptions for many microscopic process relevant to WLM rheology, from intra-tube Rouse fluctuations of stiff polymers to contour length fluctuations and bond-interchange rearrangement processes. We mention this at the outset because the main advantage of a stochastic model over a continuum model is its versatility and flexibility – whereas a major disadvantage is the difficulty in computing[6] the OSFT of $G(t)$ to get $G^*(\omega)$. In this section we will have to confront challenges with the OSFT, but we will have limited opportunities to highlight the versatility of the full Pointer model approach.

First, we evaluate the Pointer model with reversible scission rearrangements [34]. In Figure 7, we find that the the benchmark results of the shuffling model with $\zeta = 10$ and $\zeta = 0.1$ can be approximately reproduced with the Pointer model using $\zeta = 26$ and $\zeta = 0.6$. Figure 7 shows some differences between the Pointer model and the benchmark calculations at high frequencies, but we attribute this to numerical challenges with computing the OSFT and not physical differences between the models. In practice, these numerical challenges are less important once intra-tube Rouse modes dominate $G^*(\omega)$ at high frequencies.

Next, we evaluate the Pointer model with end-attack rearrangements [60]. In Figure 8, we find that the benchmark results of the shuffling model with $\zeta = 10$ and $\zeta = 0.1$ can be approximately reproduced with the end-attack Pointer model using $\zeta = 39$ and $\zeta = 0.6$.

Finally, we compare our benchmark shuffling calculations against the Pointer model for reversible scission, but now with a 'double reptation' transformation of the relaxation modulus $G(t)$ [34, 74]. This changes the modelling of the reptation sector, but leaves the rearrangement kinetics unchanged. In Figure 9, we find that the benchmark results of the shuffling model with $\zeta = 10$ and $\zeta = 0.1$ can be approximately reproduced with the double reptation Pointer model using $\zeta = 5.5$ and $\zeta = 0.18$.

Despite significant changes in the set of underlying assumptions and approximations, the various types of Pointer model for reptation and rearrangement are evidently not distinct from the shuffling model or various Poisson renewal models considered in section 4. In all cases, the models can be

[6] In practice there is a vast range of tools from traditional signal processing that have been developed to numerically approximate an OSFT operation, but in principle the problem is fundamentally ill-posed due to the ambiguity in regularization [70, 71, 72, 73].

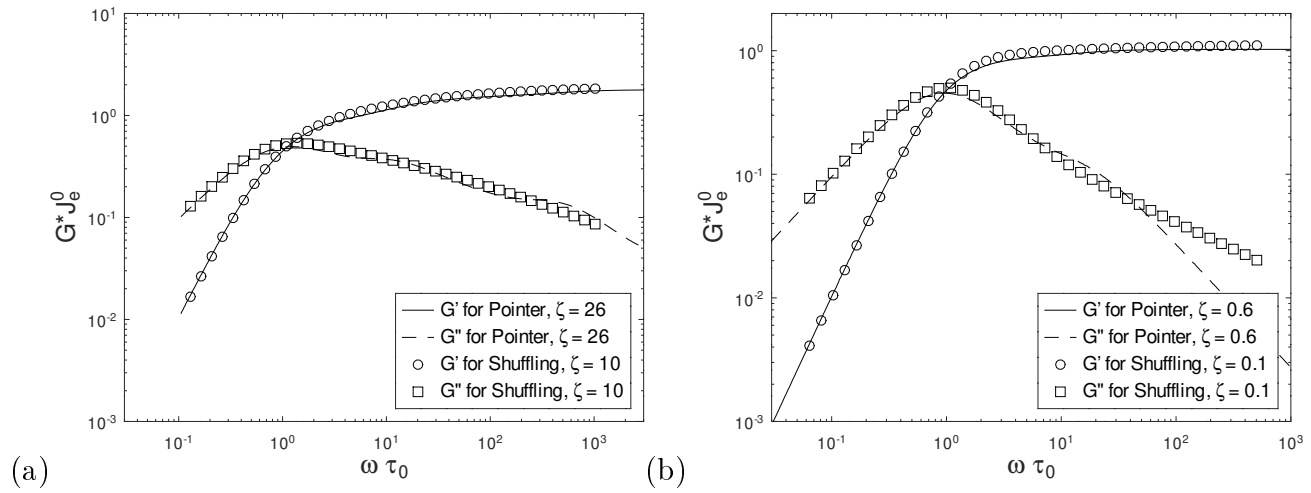

Figure 7: Comparing predictions of the Pointer model with reversible scission against the benchmark calculations of the shuffling model with (a) $\zeta = 10$ and (b) $\zeta = 0.1$, cf. Figure 3. There is no major distinction, apart from the differing fitted value of ζ in the Pointer model. We also note some oscillations in the loss modulus for the Pointer method, which we attribute to difficulties in computing an OSFT. The inability to accurately resolve G'' at high frequencies is likely responsible for other overall fitting discrepancies.

made to almost coincide within their predictive ranges for linear rheology, given suitable choices of model parameters such as ζ (which then depend strongly on the model chosen).

6 Shuffling with Double Reptation

Double reptation is a simple, and often successful, approximation strategy for dealing with the problem of thermal constraint release in well-entangled polymer melts [75, 69]. For polydisperse systems of entangled and unbreakable polymers, the double reptation and single reptation approximations generally lead to distinct rheological predictions for the same input molecular weight distribution [74]. It is therefore surprising that in section 5, the choice of single vs double reptation within a Pointer model for WLMs can be absorbed into a shift of the fitted parameters. This probably comes from the fact that double reptation and single reptation are not very distinct for systems whose rearrangements are much faster than reptation (single mode Maxwell) or much slower (unbreakable chains with exponential polydispersity).

All the same, a skeptical reader might wonder if distinct features do emerge at intermediate ζ, but have been misattributed to artifacts of the OSFT problem in Figure 9. This question can be resolved thanks to a recently developed continuum model implementation for double reptation, using a generalization of the shuffling model [23] to avoid the OSFT problem. In Figure 10, we show that the benchmark results of the single reptation shuffling model with $\zeta = 10$ and $\zeta = 0.1$ can be approximately reproduced with the double reptation shuffling model using $\zeta = 2$ and $\zeta = 0.025$.

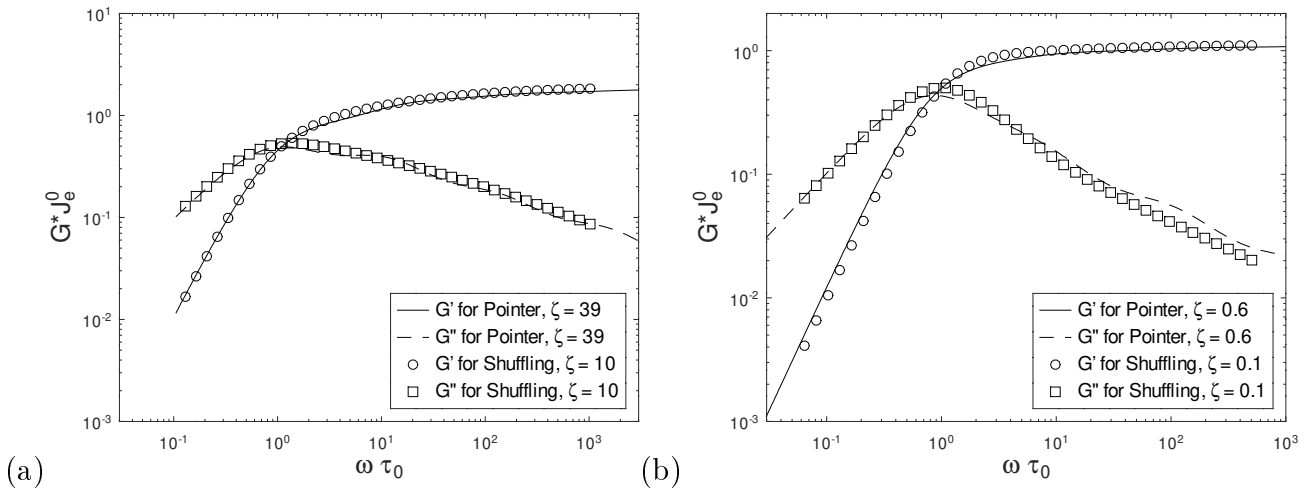

Figure 8: Comparing predictions of the Pointer model with end attack against the benchmark calculations of the shuffling model with (a) $\zeta = 10$ and (b) $\zeta = 0.1$, cf. Figure 3.

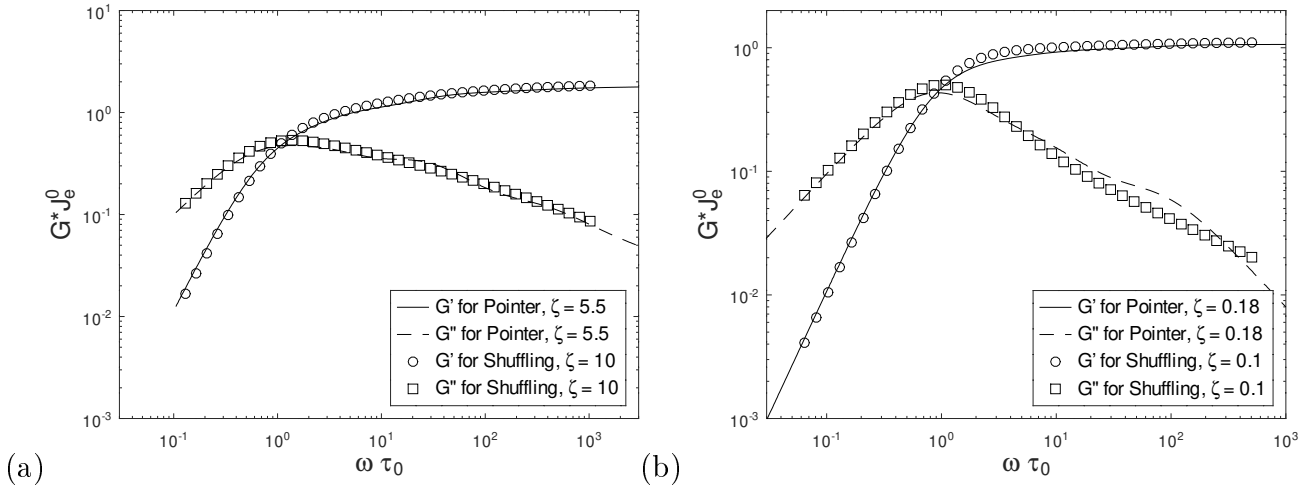

Figure 9: Comparing predictions of the Pointer model with double reptation against the benchmark calculations of the shuffling model with (a) $\zeta = 10$ and (b) $\zeta = 0.1$, cf. Figure 3.

For the fast breaking system, the transition out of a single mode Maxwell response around $\omega\tau_B \sim 1$ is very slightly broader for the double reptation approximation, but this feature is likely too subtle to be noticed in any comparison with experimental data. For the comparisons at both low and high ζ, double reption will use smaller values of ζ because reptation dynamics are sped up and a faster breaking time is needed to maintain the same ratio of timescales for stress relaxation and rearrangement.

From this comparison we conclude that the choice of double vs single reptation in a WLM model modulates the fitting of model parameters but does not otherwise alter predictions in a distinct way. Moreover, the reduction in fitted ζ from single to double reptation is consistent with what was seen from the Pointer model, cf. Figures 9 and 7.

For a more complete treatment of constraint release, a different class of constitutive modeling

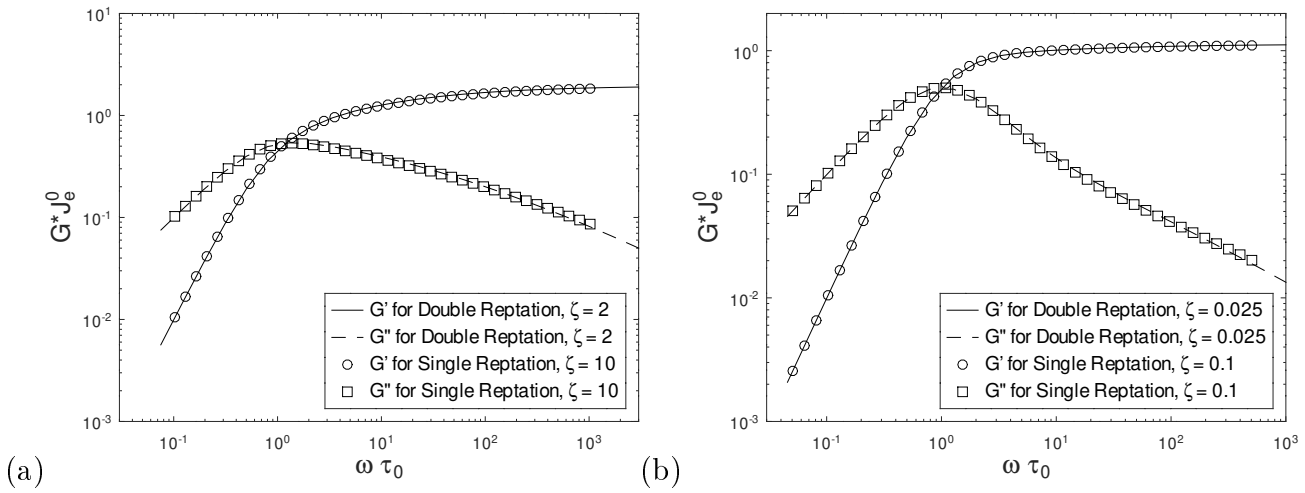

Figure 10: Comparing predictions of the double reptation shuffling model against the single reptation shuffling model with (a) $\zeta = 10$ and (b) $\zeta = 0.1$, cf. Figure 3.

framework is required in order to resolve the full Rouse-like motion of the tube itself. These ideas have been previously incorporated into population balance constitutive models for wormlike micelles [39], but the resulting model predictions were marred by issues that arose from replacing a discrete Rouse spectra with a continuous approximation.

7 Intra-tube Rouse Modes and Feature-Parameter Mapping

Up to this point, we have neglected intra-tube Rouse modes (i.e. Rouse modes having a wavelength no longer than the tube diameter) and consequently none of our figures have included the characteristic upturn in the loss modulus seen at high frequencies [76, 77]. This section reviews a simple and approximate way of incorporating intra-tube Rouse modes. We also discuss the relationship between "features" of linear rheology measurements and "parameters" of a fitted model (i.e. feature-parameter mapping). This is useful for anticipating (1) what information might be present in a given set of linear rheology data and (2) what information might be missing or best measured by some other means.

7.1 Intra-tube dynamics

We will assume that WLMs are very flexible on scales comparable to the tube diameter, such that the complex modulus from intra-tube Rouse modes $G_R^*(\omega)$ is given by the Rouse model [51, 78]:

$$G_R^*(\omega) = G_e \int_0^\infty dZ \phi(Z) \frac{1}{Z} \sum_{p=Z}^{N_e Z} \frac{i\omega\tau_e/2}{i\omega\tau_e/2 + (p/Z)^2} \tag{23}$$

where $Z = L/L_e$ is an entanglement number, τ_e is the longest Rouse time for an entanglement segment, $\phi(Z)$ is the the length distribution of the WLMs, and N_e is the number of Kuhn segments per entanglement section. If the WLMs are very flexible on the scale of an entanglement segment, $N_e \gg 1$, the above sum approximately evaluates to:

$$G_R^*(\omega) \approx G_e \int_0^\infty dZ\phi(Z)\sqrt{\frac{i\omega\tau_e}{2}}\arctan\left[\sqrt{\frac{i\omega\tau_e}{2}}\right] = G_e\sqrt{\frac{i\omega\tau_e}{2}}\arctan\left[\sqrt{\frac{i\omega\tau_e}{2}}\right] \tag{24}$$

These assumptions and approximations on flexibility may not be reflected in real systems, but they are useful here for pedagogical purposes. Many WLM systems will be semi-flexible or stiff, in which case additional physics is needed to describe the rheology above $\omega > 1/\tau_e$ [34, 54]. With this minimal set of physics, Rouse modes introduce a new parameter - the entanglement Rouse time τ_e. From reptation theory, τ_e should be related to the reptation time $\bar{\tau}_{\text{rep}}$ via the entanglement number of a typical chain, $\bar{Z}$, with $\bar{\tau}_{\text{rep}} = 3\bar{Z}^3\tau_e$. Thus, the Rouse modes can also be seen as adding information about the entanglement number if $\bar{\tau}_{\text{rep}}$ is known or included as a fitting parameter for the low frequency rheology.

If we add $G_R^*(\omega)$ from the intra-tube Rouse modes to the complex modulus from the shuffling model, we get the overall complex modulus shown in Figure 11. These calculations specify an average entanglement number of $\bar{Z} = 30$. For larger values of $\bar{Z}$, the intra-tube Rouse modes are shifted to higher frequencies. We note that for lower entanglement numbers $\bar{Z} < 10$, inclusion of slower Rouse modes corresponding to wavelengths longer than an entanglement spacing have been found necessary to correctly match the rheology predicted by the more microscopic slip-spring model [67].

7.2 Feature-parameter mapping

When fitting models to experimental data, it is important to choose models that provide the right level of physical insight. For example, if intra-tube Rouse modes are not clearly evidenced in the linear rheology data, as detailed below, the entanglement time τ_e should not be included as a fitting parameter; including it can lead to overfitting or slow/unstable convergence in the fitting algorithm. In some respects, this is common sense, but for complicated models it is not always obvious what information is represented in the data before conducting a thorough comparison with a model.

This subsection aims to provide heuristics that anticipate whether an experimental data set contains sufficient information to specify a parameter or whether that parameter must be measured independently by some other means.

For this subsection, we define the 'low frequency' and 'high frequency' rheology in relation to

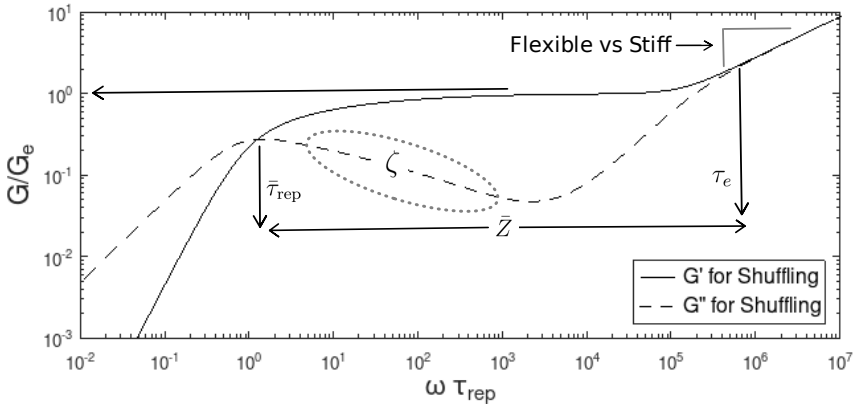

Figure 11: Predictions for the complex modulus $G^*(\omega)$ of a very flexible WLM with $\zeta = 10$ and $\bar{Z} = 30$, including intra-tube Rouse modes via equation 24. At frequencies above $\omega\bar{\tau}_{\rm rep} > 10^3$, the intra-tube Rouse modes dominate the loss modulus, and at frequencies above $\omega\bar{\tau}_{\rm rep} > 10^5$ they dominate the storage modulus as well. Superimposed upon these curves are *schematic* indicators for feature-parameter mapping, cf. section 7.2. The crossover frequency does not equal the reptation time $\bar{\tau}_{\rm rep}$ but it does provide information needed to ascertain $\bar{\tau}_{\rm rep}$. Likewise the separation between $\bar{\tau}_{\rm rep}$ and τ_e provides information needed to determine $\bar{Z}$ but is not equal to $\bar{Z}$. For the model fit to be well-posed, the experimental data must contain enough distinct features to specify all model parameters.

the freqency $\omega_{\rm min}$, at which a local minimum appears in the loss modulus. For WLMs relaxing by reptation and intra-tube Rouse rearrangement, some model parameters can be found through the low frequency rheology, some can be found from the high frequency rheology, and some can only be found when combining both the high and low frequency model parameters.

As a disclaimer, our discussion on feature-parameter-mapping excludes the effects of contour length fluctuations, which in principle can provide a second independent means of estimating the entanglement number $\bar{Z}$ [55]. However, for an imperfect model it is possible that different model-based comparisons or heuristics will generate conflicting estimates of the entanglement number. Resolving such a conflict is more of an art than a science, and it goes beyond the scope of what we are able to cover here. The signature from contour length fluctuations enters in the low-to-intermediate frequency range, and CLF is not strictly necessary for feature-parameter mapping provided the system is very well entangled and not too fast breaking, $\zeta > 1/\bar{Z}$.

In broad conceptual terms, we have seen that the 'shape' of the low frequency response is governed by a single dimensionless parameter[7] ζ, which compares an effective relaxation time to the characteristic time for some underlying stress relaxation process. Seeing this universality, the low-frequency response involves only three parameters for a complete classification - a shear modulus G_e, a long relaxation time (e.g. $\bar{\tau}_{\rm rep}$), and some general shape parameter, $\bar{\zeta}$. The linear rheology

[7]This is true provided the WLMs are well-entangled and flexible/semiflexible with $\zeta \gg 1/\bar{Z}$. For very small values of ζ, both ζ and $\bar{Z}$ are needed to describe the low frequency response due to the dominant role of contour length fluctuations [23].

data in the low frequency range does not contain information beyond these three parameters, and the value assigned to those parameters will depend on the model used. If a general shape parameter $\bar{\zeta}$ is not enough for a useful interpretation of the experimental data (i.e if the specific choice of rearrangment pathway really matters) then the low frequency rheology data can provide an estimate of ζ for a *specified* rearrangment pathway, but the low frequency rheology cannot also independently corroborate the *choice* of rearrangement pathway. To corroborate a rearrangement pathway, additional experiments are needed, which can include include some combination of:

1. High frequency rheology: At high frequencies, contour length fluctuations and intra-tube Rouse modes provide information about the entanglement number [55, 53, 79, 80] and WLM stiffness [54, 34, 81, 82]. Information about the entanglement number also allows an estimate of the WLM scission energy [34, 83, 84] given a specified rearrangement pathway. The high frequency response does *not* differentiate between rearrangement pathways.

2. Temperature-jump: A rapid temperature change will cause the molecular weight distribution to fall out of equilibrium. Scattering or rheological measurements taken along the path to equilibration can reveal the natural time-scales associated with specific rearrangement pathways [85, 86, 87]. In principle, the molecular weight distribution can also be perturbed from equilibrium by non-linear rheology to facilitate the same kind of measurements, but this has not been fully explored [62, 63].

3. Other non-rheological measurements: Additional information about the structure and dynamics of a WLM system can be obtained from a great variety of methods including conductivity [88, 89]; neutron and light scattering [90, 91, 92, 93]; cryo-TEM [94, 95, 96, 97]; and molecular dynamics simulations [98, 99, 100, 101].

Information from (2) and (3) go beyond the narrow focus of this paper, but regarding (1) we can note the value of high frequency linear rheology data, which provides two main pieces of information: First, it reveals the longest intra-tube Rouse relaxation time, τ_e. In conjunction with an estimation for $\bar{\tau}_{\text{rep}}$ (which can be estimated via the low frequency rheology), τ_e can be used to estimate an entanglement number $\bar{Z}$. Second, for frequencies above $\omega > 1/\tau_e$, the scaling laws for loss modulus and shear modulus can reveal information about chain stiffness [54, 102, 103]. In conjunction with estimates for G_e and $\bar{\tau}_{\text{rep}}$, the high frequency rheology can provide improved estimates of entanglement lengths and entanglement numbers [34].

The overall feature-parameter mapping strategy is summarized schematically in Figure 11, where annotations identify features that provide information but do not imply one-to-one mappings (i.e. the low frequency crossover is not $1/\bar{\tau}_{\text{rep}}$). The Pointer model is currently the most complete modeling framework for detailed feature-parameter mapping in WLM, incorporating additional

models and correlations beyond those outlined here. In particular, the Pointer model includes correlations to infer microscopic properties (e.g., scission energy and the entanglement length) from the entanglement number $\bar{Z}$ and the plateau modulus G_e; see for example [34].

8 Summary and Future Directions

This work summarizes a series of advances, spanning several decades, in modeling the linear rheology of WLMs by combining the physics of reptation (diffusion) and sequence rearrangement (breaking and reformation of chains). Specifically, we address three modeling frameworks - the Poisson renewal model, the Pointer model, and the shuffling model - that all aim to describe reversible scission and reptation but employ differing assumptions and approximation schemes, balancing constraints on computational speed, robustness, and accuracy. In practice, these models are designed for the purpose of fitting and interpreting linear rheology data on WLMs, and in the end we find that none of the models is distinct from the others for the purpose of this aim. In other words, the shape of the complex modulus $G^*(\omega)$ can be reliably fitted by any of the models, and all that differs is the fitted parameter values. This result is both disappointing and encouraging. It is disappointing because it suggest that a good fit to experimental data obtained with a reversible scission model does not necessarily corroborate the assumption of a reversible scission rearrangement pathway – an equally good fit could be obtained by shuffling or Poisson renewal. To validate a sequence rearrangement pathway requires additional information outside of linear rheology (cf. subsection 7.2), and such information is often slow and expensive to acquire by comparison. However, for industrial applications a fast qualitative assessment may often be preferable to a slow quantitative assessment. In such cases, our findings should be encouraging - the fastest models are just as useful as the most detailed models for qualitative assessments.

For rapid qualitative parameter assessments and predictable fitting at all frequencies, our study recommends a shuffling model. Alternatively, for optimal quantitative parameter estimation with known sequence rearrangement pathways, one can use the Pointer modeling framework. If additional work is done on modeling the linear rheology of wormlike micelles undergoing reptation and rearrangement (to the exclusion of all other processes), the main value would lie in resolving questions *beyond* the fitting of linear rheology data, such as parameterizing a non-linear rheology model.

At the same time, reptation is not the only rheologically meaningful tube-scale process in highly entangled WLM systems. There are other non-separable and distinctive linear relaxation mechanisms (contour length fluctuations, thermal constraint release), plus additional WLM architectures (loops, branches, networks) to be considered, all of which were neglected in the present study. In general the full complexity of WLM rheology should not be *expected* to collapse onto a small

number of parameters as we found in this work; as new physics are incorporated, new distinctions may emerge. However, early evidence suggests that a 'principle of equivalence' in WLM rheology could be surprisingly universal; a forthcoming publication will show that branched WLMs can be modeled as linear WLMs, given an appropriate correction to the average micelle length [40].

In future research there are many open directions worth pursuing, especially insofar as WLMs are a 'model polymer' system for studying fundamental questions in entangled polymer rheology. Improved WLM models could provide valuable new insights on marginally entangled polymer rheology [61], flow-induced disentanglement [104], and convective constraint release [69, 39, 105]. For systems far from equilibrium, WLMs may also serve as a model system for studying fundamental questions relevant to polymer recycling (e.g. chemolysis, thermolysis, reactive compatibilization, reactive extrusion). Finally, there are opportunities to continue integrating population balance equations into an expanded range of complex fluids applications, from suspension crystallization to aggregation/breakup phenomena in gels and emulsions.

Acknowledgments: Funding for RGL was provided by the National Science Foundation under grant CBETÂ 2323147. Any opinions, findings, and conclusions or recommendations expressed in this material are those of the authors and do not necessarily reflect the views of NSF. MEC was funded by the Royal Society.

References

[1] Francois Lequeux. "Structure and rheology of wormlike micelles". In: *Current Opinion in Colloid & Interface Science* 1.3 (1996), pp. 341–344.

[2] Florian Nettesheim and Eric W Kaler. "Phase behavior of systems with wormlike micelles". In: *Giant Micelles*. CRC Press, 2007, pp. 223–248.

[3] M. Jayne Lawrence. "Surfactant systems: their use in drug delivery". In: *Chem. Soc. Rev.* 23 (6 1994), pp. 417–424.

[4] John F. Scamehorn. *An overview of phenomena involving surfactant mixtures*. ACS publications, 1986. Chap. 1, pp. 1–27.

[5] Iva Kralova and Johan Sjoblom. "Surfactants used in food industry: A review". In: *Journal of Dispersion Science and Technology* 30.9 (2009), pp. 1363–1383.

[6] M. Rosen. *Surfactants and interfacial phenomena, second edition*. Vol. 94. 7. John Wiley & Sons Ltd, New York, 1990, pp. 796–796.

[7] Geoffrey Maitland. "Oil and gas production". In: *Current Opinion in Colloid and Interface Science* 5 (2000), pp. 301–311.

[8] SJ Candau, A Khatory, F Lequeux, and F Kern. "Rheological behaviour of wormlike micelles: effect of salt content". In: *Le Journal de Physique IV* 3.C1 (1993), pp. C1–197.

[9] Z Lin, JJ Cai, LE Scriven, and HT Davis. "Spherical-to-wormlike micelle transition in CTAB solutions". In: *The Journal of Physical Chemistry* 98.23 (1994), pp. 5984–5993.

[10] PA Hassan, SJ Candau, F Kern, and C Manohar. "Rheology of wormlike micelles with varying hydrophobicity of the counterion". In: *Langmuir* 14.21 (1998), pp. 6025–6029.

[11] Alan Parker and Wolfgang Fieber. "Viscoelasticity of anionic wormlike micelles: effects of ionic strength and small hydrophobic molecules". In: *Soft Matter* 9.4 (2013), pp. 1203–1213.

[12] Jiang Yang. "Viscoelastic wormlike micelles and their applications". In: *Current opinion in colloid & interface science* 7.5-6 (2002), pp. 276–281.

[13] Linda D Rhein, Mitchell Schlossman, Anthony O'Lenick, and P Somasundaran. *Surfactants in personal care products and decorative cosmetics*. Vol. 135. crc press, 2006.

[14] Trang Vu, Peter Koenig, Mike Weaver, Howard D. Hutton, and Gerald B. Kasting. "Effects of cationic counterions and surfactant on viscosity of an amino acid-based surfactant system". In: *Colloids and Surfaces A: Physicochemical and Engineering Aspects* 626 (2021), p. 127040. ISSN: 0927-7757.

[15] ME Cates. "Reptation of living polymers: dynamics of entangled polymers in the presence of reversible chain-scission reactions". In: *Macromolecules* 20.9 (1987), pp. 2289–2296.

[16] R Granek and ME Cates. "Stress relaxation in living polymers: Results from a Poisson renewal model". In: *The Journal of chemical physics* 96.6 (1992), pp. 4758–4767.

[17] Lynn M Walker, Paula Moldenaers, and Jean-François Berret. "Macroscopic response of wormlike micelles to elongational flow". In: *Langmuir* 12.26 (1996), pp. 6309–6314.

[18] Jean-François Berret, Grégoire Porte, and Jean-Paul Decruppe. "Inhomogeneous shear flows of wormlike micelles: A master dynamic phase diagram". In: *Physical Review E* 55.2 (1997), p. 1668.

[19] Richard D Koehler, Srinivasa R Raghavan, and Eric W Kaler. "Microstructure and dynamics of wormlike micellar solutions formed by mixing cationic and anionic surfactants". In: *The Journal of Physical Chemistry B* 104.47 (2000), pp. 11035–11044.

[20] Matthew E Helgeson, Paula A Vasquez, Eric W Kaler, and Norman J Wagner. "Rheology and spatially resolved structure of cetyltrimethylammonium bromide wormlike micelles through the shear banding transition". In: *Journal of Rheology* 53.3 (2009), pp. 727–756.

[21] Zuowei Wang and Ronald G Larson. "Molecular dynamics simulations of threadlike cetyltrimethylammonium chloride micelles, effects of sodium chloride and sodium salicylate salts". In: *The Journal of Physical Chemistry B* 113.42 (2009), pp. 13697–13710.

[22] Zonglin Chu, Cécile A Dreiss, and Yujun Feng. "Smart wormlike micelles". In: *Chemical Society Reviews* 42.17 (2013), pp. 7174–7203.

[23] JD Peterson and ME Cates. "Constitutive models for well-entangled living polymers beyond the fast-breaking limit". In: *Journal of Rheology* 65.4 (2021), pp. 633–662.

[24] Patrick J McCauley, Satish Kumar, and Michelle A Calabrese. "Criteria governing rod formation and growth in nonionic polymer micelles". In: *Langmuir* 37.40 (2021), pp. 11676–11687.

[25] H Rehage and HJMP Hoffmann. "Viscoelastic surfactant solutions: model systems for rheological research". In: *Molecular Physics* 74.5 (1991), pp. 933–973.

[26] Danila Gaudino, Salvatore Costanzo, Giovanni Ianniruberto, Nino Grizzuti, and Rossana Pasquino. "Linear wormlike micelles behave similarly to entangled linear polymers in fast shear flows". In: *Journal of Rheology* 64.4 (2020), pp. 879–888.

[27] Jonathan P Rothstein and Hadi Mohammadigoushki. "Complex flows of viscoelastic wormlike micelle solutions". In: *Journal of Non-Newtonian Fluid Mechanics* 285 (2020), p. 104382.

[28] Sandra Lerouge. "Flow of wormlike micelles: From shear banding to elastic turbulence". In: *Science Talks* 3 (2022), p. 100050.

[29] Hugo A Castillo Sánchez, Mihailo R Jovanovic, Satish Kumar, Alexander Morozov, V Shankar, Ganesh Subramanian, and Helen J Wilson. "Understanding viscoelastic flow instabilities: Oldroyd-B and beyond". In: *Journal of Non-Newtonian Fluid Mechanics* (2022), p. 104742.

[30] Ben O'Shaughnessy. "From mean field to diffusion-controlled kinetics: Concentration-induced transition in reacting polymer solutions". In: *Phys. Rev. Lett.* 71 (20 1993), pp. 3331–3334.

[31] E. A. G. Aniansson and S. N. Wall. "Kinetics of step-wise micelle association". In: *The Journal of Physical Chemistry* 78.10 (1974), pp. 1024–1030.

[32] Michael E Cates and Suzanne M Fielding. "Rheology of giant micelles". In: *Advances in Physics* 55.7-8 (2006), pp. 799–879.

[33] I. A. Babintsev, L. Ts. Adzhemyan, and A. K. Shchekin. "Kinetics of micellisation and relaxation of cylindrical micelles described by the difference BeckerâDoring equation". In: *Soft Matter* 10 (15 2014), pp. 2619–2631.

[34] Weizhong Zou and Ronald G Larson. "A mesoscopic simulation method for predicting the rheology of semi-dilute wormlike micellar solutions". In: *Journal of Rheology* 58.3 (2014), pp. 681–721.

[35] Sylvio May, Yardena Bohbot, and Avinoam Ben-Shaul. "Molecular theory of bending elasticity and branching of cylindrical micelles". In: *The Journal of Physical Chemistry B* 101.43 (1997), pp. 8648–8657.

[36] Niti R. Agrawal, Xiu Yue, and Srinivasa R. Raghavan. "The unusual rheology of wormlike micelles in glycerol: comparable timescales for chain reptation and segmental relaxation". In: *Langmuir* 36.23 (2020), pp. 6370–6377.

[37] Prasuna Koshy, V. K. Aswal, Meera Venkatesh, and P. A. Hassan. "Unusual scaling in the rheology of branched wormlike micelles formed by cetyltrimethylammonium bromide and sodium oleate". In: *The Journal of Physical Chemistry B* 115.37 (2011), pp. 10817–10825.

[38] T. Imae and S. Ikeda. "Characteristics of rodlike micelles of cetyltrimethylammonium chloride in aqueous NaCl solutions: Their flexibility and the scaling laws in dilute and semidilute regimes". In: *Colloid and Polymer Science* 265 (1987), pp. 1090–1098.

[39] Joseph D Peterson and ME Cates. "A full-chain tube-based constitutive model for living linear polymers". In: *Journal of Rheology* 64.6 (2020), pp. 1465–1496.

[40] Weizhong Zou, Grace Tan, Mike Weaver, Peter Koenig, and Ronald G. Larson. "Mesoscopic modeling of the effect of branching on the viscoelasticity of entangled wormlike micellar solutions". In: *under review, Physical Review Research* (2023).

[41] R Messager, A Ott, D Chatenay, W Urbach, and D Langevin. "Are giant micelles living polymers?" In: *Physical review letters* 60.14 (1988), p. 1410.

[42] Zhihu Yan, Caili Dai, Mingwei Zhao, and Yongpeng Sun. "Rheological characterizations and molecular dynamics simulations of self-assembly in an anionic/cationic surfactant mixture". In: *Soft Matter* 12 (28 2016), pp. 6058–6066.

[43] Jacob N. Israelachvili, D. John Mitchell, and Barry W. Ninham. "Theory of self-assembly of hydrocarbon amphiphiles into micelles and bilayers". In: *J. Chem. Soc., Faraday Trans. 2* 72 (0 1976), pp. 1525–1568.

[44] Kenichi Eguchi, Isamu Kaneda, Yoshiko Hiwatari, Hiroyasu Masunaga, and Kazuo Sakurai. "Salt-concentration dependence of the structure and form factors for the wormlike micelle made from a dual surfactant in aqueous solutions". In: *Journal of Applied Crystallography* 40.s1 (2007), s264–s268.

[45] Norio Nemoto, Mitsue Kuwahara, Ming-L. Yao, and Kunihiro Osaki. "Dynamic Light Scattering of CTAB/NaSal Threadlike Micelles in a Semidilute Regime. 3. Dynamic Coupling between Concentration Fluctuation and Stress". In: *Langmuir* 11.1 (1995), pp. 30–36.

[46] Pierre-Giles De Gennes. "Reptation of a polymer chain in the presence of fixed obstacles". In: *The journal of chemical physics* 55.2 (1971), pp. 572–579.

[47] Masao Doi and SF Edwards. "Dynamics of concentrated polymer systems. Part 3.âThe constitutive equation". In: *Journal of the Chemical Society, Faraday Transactions 2: Molecular and Chemical Physics* 74 (1978), pp. 1818–1832.

[48] MS Turner and ME Cates. "Linear viscoelasticity of living polymers: A quantitative probe of chemical relaxation times". In: *Langmuir* 7.8 (1991), pp. 1590–1594.

[49] Charles L Epstein and John Schotland. "The bad truth about Laplace's transform". In: *SIAM review* 50.3 (2008), pp. 504–520.

[50] ME Cates. "Theory of the viscosity of polymeric liquid sulfur". In: *Europhysics Letters* 4.4 (1987), p. 497.

[51] Masao Doi, Samuel Frederick Edwards, and Samuel Frederick Edwards. *The theory of polymer dynamics*. Vol. 73. Oxford University Press, 1988.

[52] Ben O'Shaughnessy and Jane Yu. "Rheology of wormlike micelles: two universality classes". In: *Phys. Rev. Lett.* 74 (21 1995), pp. 4329–4332.

[53] Grace Tan, Weizhong Zou, Mike Weaver, and Ronald G Larson. "Determining threadlike micelle lengths from rheometry". In: *Journal of Rheology* 65.1 (2021), pp. 59–71.

[54] David C Morse. "Viscoelasticity of concentrated isotropic solutions of semiflexible polymers. 2. Linear response". In: *Macromolecules* 31.20 (1998), pp. 7044–7067.

[55] Rony Granek. "Dip in G" of polymer melts and semidilute solutions". In: *Langmuir* 10.5 (1994), pp. 1627–1629.

[56] Suliman Barhoum, Rolando Castillo, and A Yethiraj. "Characterization of dynamics and internal structure of a mixed-surfactant wormlike micellar system using NMR and rheometry". In: *Soft Matter* 8 (26 2012), pp. 6950–6957.

[57] Florian Nettesheim and Norman J. Wagner. "Fast dynamics of wormlike micellar solutions". In: *Langmuir* 23.10 (2007), pp. 5267–5269.

[58] C. Oelschlaeger, M. Schopferer, F. Scheffold, and N. Willenbacher. "Linear-to-branched micelles transition: a rheometry and diffusing wave spectroscopy (DWS) study". In: *Langmuir* 25.2 (2009), pp. 716–723.

[59] F Lequeux. "Linear response of self assembling systems: mean field solution". In: *Journal de Physique II* 1.2 (1991), pp. 195–207.

[60] Weizhong Zou, Xueming Tang, Mike Weaver, Peter Koenig, and Ronald G Larson. "Determination of characteristic lengths and times for wormlike micelle solutions from rheology using a mesoscopic simulation method". In: *Journal of Rheology* 59.4 (2015), pp. 903–934.

[61] Takeshi Sato, Soroush Moghadam, Grace Tan, and Ronald G Larson. "A slip-spring simulation model for predicting linear and nonlinear rheology of entangled wormlike micellar solutions". In: *Journal of Rheology* 64.5 (2020), pp. 1045–1061.

[62] Joseph D Peterson and L Gary Leal. "Predictions for flow-induced scission in well-entangled living polymers: The living Rolie-Poly model". In: *Journal of Rheology* 65.5 (2021), pp. 959–982.

[63] Paula A Vasquez, Gareth H McKinley, and L Pamela Cook. "A network scission model for wormlike micellar solutions: I. Model formulation and viscometric flow predictions". In: *Journal of non-newtonian fluid mechanics* 144.2-3 (2007), pp. 122–139.

[64] Natalie Germann, LP Cook, and Antony N Beris. "Nonequilibrium thermodynamic modeling of the structure and rheology of concentrated wormlike micellar solutions". In: *Journal of Non-Newtonian Fluid Mechanics* 196 (2013), pp. 51–57.

[65] Deepa M Nair and Jay D Schieber. "Linear viscoelastic predictions of a consistently unconstrained Brownian slip-link model". In: *Macromolecules* 39.9 (2006), pp. 3386–3397.

[66] Silabrata Pahari, Bhavana Bhadriraju, Mustafa Akbulut, and Joseph Sang-Il Kwon. "A slip-spring framework to study relaxation dynamics of entangled wormlike micelles with kinetic Monte Carlo algorithm". In: *Journal of Colloid and Interface Science* 600 (2021), pp. 550–560.

[67] Grace Tan and Ronald G Larson. "Quantitative modeling of threadlike micellar solution rheology". In: *Rheologica Acta* 61.7 (2022), pp. 443–457.

[68] NA Spenley, ME Cates, and TCB McLeish. "Nonlinear rheology of wormlike micelles". In: *Physical review letters* 71.6 (1993), p. 939.

[69] ST Milner, TCB McLeish, and AE Likhtman. "Microscopic theory of convective constraint release". In: *Journal of Rheology* 45.2 (2001), pp. 539–563.

[70] Ian McDougall, Nese Orbey, and John M Dealy. "Inferring meaningful relaxation spectra from experimental data". In: *Journal of Rheology* 58.3 (2014), pp. 779–797.

[71] Sayali R Kedari, Gowtham Atluri, and Kumar Vemaganti. "A hierarchical Bayesian approach to regularization with application to the inference of relaxation spectra". In: *Journal of Rheology* 66.1 (2022), pp. 125–145.

[72] Y Leong Yeow, Woan C Ko, and Pannie PP Tang. "Solving the inverse problem of Couette viscometry by Tikhonov regularization". In: *Journal of Rheology* 44.6 (2000), pp. 1335–1351.

[73] Yufei Wei, Michael J Solomon, and Ronald G Larson. "Quantitative nonlinear thixotropic model with stretched exponential response in transient shear flows". In: *Journal of Rheology* 60.6 (2016), pp. 1301–1315.

[74] J Des Cloizeaux. "Double reptation vs. simple reptation in polymer melts". In: *Europhysics Letters* 5.5 (1988), p. 437.

[75] Jean Louis Viovy, Michael Rubinstein, and Ralph H Colby. "Constraint release in polymer melts: Tube reorganization versus tube dilation". In: *Macromolecules* 24.12 (1991), pp. 3587–3596.

[76] M Buchanan, M Atakhorrami, JF Palierne, FC MacKintosh, and CF Schmidt. "High-frequency microrheology of wormlike micelles". In: *Physical Review E* 72.1 (2005), p. 011504.

[77] C Oelschlaeger, P Suwita, and N Willenbacher. "Effect of counterion binding efficiency on structure and dynamics of wormlike micelles". In: *Langmuir* 26.10 (2010), pp. 7045–7053.

[78] Prince E Rouse Jr. "A theory of the linear viscoelastic properties of dilute solutions of coiling polymers". In: *The Journal of Chemical Physics* 21.7 (1953), pp. 1272–1280.

[79] Toyoko Imae and Shoichi Ikeda. "Sphere-rod transition of micelles of tetradecyltrimethylammonium halides in aqueous sodium halide solutions and flexibility and entanglement of long rodlike micelles". In: *The Journal of Physical Chemistry* 90.21 (1986), pp. 5216–5223.

[80] A. Khatory, F. Kern, F. Lequeux, J. Appell, G. Porte, N. Morie, A. Ott, and W. Urbach. "Entangled versus multiconnected network of wormlike micelles". In: *Langmuir* 9.4 (1993), pp. 933–939.

[81] N. Willenbacher, C. Oelschlaeger, M. Schopferer, P. Fischer, F. Cardinaux, and F. Scheffold. "Broad bandwidth optical and mechanical rheometry of wormlike micelle solutions". In: *Phys. Rev. Lett.* 99 (6 2007), p. 068302.

[82] Dirk Sachsenheimer, Claude Oelschlaeger, Sonja Muller, Jan Kustner, Sebastian Bindgen, and Norbert Willenbacher. "Elongational deformation of wormlike micellar solutions". In: *Journal of Rheology* 58.6 (2014), pp. 2017–2042.

[83] Isabelle Couillet, Trevor Hughes, Geoffrey Maitland, Francoise Candau, and S. Jean Candau. "Growth and scission energy of wormlike micelles formed by a cationic surfactant with long unsaturated tails". In: *Langmuir* 20.22 (2004), pp. 9541–9550.

[84] E. Faetibold, B. Michels, and G. Waton. "Micellar growth study by microcalorimetry in CTAB solutions". In: *The Journal of Physical Chemistry* 100.51 (1996), pp. 20063–20067.

[85] MS Turner and ME Cates. "The relaxation spectrum of polymer length distributions". In: *Journal de Physique* 51.4 (1990), pp. 307–316.

[86] Gokul C. Kalur, Bradley D. Frounfelker, Bani H. Cipriano, Alexander I. Norman, and Srinivasa R. Raghavan. "Viscosity increase with temperature in cationic surfactant solutions due to the growth of wormlike micelles". In: *Langmuir* 21.24 (2005), pp. 10998–11004.

[87] E. Cappelaere, Robert Cressely, R. Makhloufi, and J. P. Decruppe. "Temperature and flow-induced viscosity transitions for CTAB surfactant solutions". In: *Rheologica Acta* 33.5 (1994), pp. 431–437.

[88] Matthew E. Helgeson, Travis K. Hodgdon, Eric W. Kaler, Norman J. Wagner, Martin Vethamuthu, and K. P. Ananthapadmanabhan. "Formation and rheology of viscoelastic double networks in wormlike micelleânanoparticle mixtures". In: *Langmuir* 26.11 (2010), pp. 8049–8060. DOI: 10.1021/la100026d.

[89] John K. Riley, Jeffrey J. Richards, Norman J. Wagner, and Paul D. Butler. "Branching and alignment in reverse worm-like micelles studied with simultaneous dielectric spectroscopy and RheoSANS". In: *Soft Matter* 14 (26 2018), pp. 5344–5355.

[90] Weizhong Zou, Grace Tan, Hanqiu Jiang, Karsten Vogtt, Michael Weaver, Peter Koenig, Gregory Beaucage, and Ronald G. Larson. "From well-entangled to partially-entangled wormlike micelles". In: *Soft Matter* 15 (4 2019), pp. 642–655.

[91] Karsten Vogtt, Gregory Beaucage, Kabir Rishi, Hanqiu Jiang, and Andrew Mulderig. "Hierarchical approach to aggregate equilibria". In: *Phys. Rev. Res.* 1 (3 Nov. 2019), p. 033081.

[92] Wyn Brown, Karin Johansson, and Mats Almgren. "Threadlike micelles from cetyltrimethylammonium bromide in aqueous sodium naphthalenesulfonate solutions studied by static and dynamic light scattering". In: *The Journal of Physical Chemistry* 93.15 (1989), pp. 5888–5894.

[93] Kenzo Naruse, Kenichi Eguchi, Isamu Akiba, Kazuo Sakurai, Hiroyasu Masunaga, Hiroki Ogawa, and John S. Fossey. "Flexibility and cross-sectional structure of an anionic dual-surfactant wormlike micelle explored with small-angle x-ray scattering coupled with contrast variation technique". In: *The Journal of Physical Chemistry B* 113.30 (2009), pp. 10222–10229.

[94] "Rheology of branched wormlike micelles". In: *Current Opinion in Colloid & Interface Science* 19.6 (2014), pp. 530–535. ISSN: 1359-0294. DOI: https://doi.org/10.1016/j.cocis.2014.10.006.

[95] Sylvio May, Yardena Bohbot, and Avinoam Ben-Shaul. "Molecular theory of bending elasticity and branching of cylindrical micelles". In: *The Journal of Physical Chemistry B* 101.43 (1997), pp. 8648–8657. DOI: 10.1021/jp971328q.

[96] Vania Croce, Terence Cosgrove, Geoff Maitland, Trevor Hughes, and Goran Karlsson. "Rheology, cryogenic transmission electron spectroscopy, and small-angle neutron scattering of highly viscoelastic wormlike micellar solutions". In: *Langmuir* 19.20 (2003), pp. 8536–8541.

[97] Dganit Danino, Yeshayahu Talmon, and Raoul Zana. "Cryo-TEM of thread-like micelles: on-the-grid microstructural transformations induced during specimen preparation". In: *Colloids and Surfaces A: Physicochemical and Engineering Aspects* 169.1 (2000), pp. 67–73.

[98] Grace Tan, Weizhong Zou, Mike Weaver, and Ronald G. Larson. "Determining threadlike micelle lengths from rheometry". In: *Journal of Rheology* 65.1 (2021), pp. 59–71. DOI: 10.1122/8.0000152.

[99] Ming Tang and W. Craig Carter. "branching mechanisms in surfactant micellar growth". In: *The Journal of Physical Chemistry B* 117.10 (2013), pp. 2898–2905. DOI: 10.1021/jp309204t.

[100] Chrystal D. Bruce, Sanjib Senapati, Max L. Berkowitz, Lalith Perera, and Malcolm D. E. Forbes. "Molecular dynamics simulations of sodium dodecyl sulfate micelle in water: the behavior of water". In: *The Journal of Physical Chemistry B* 106.42 (2002), pp. 10902–10907.

[101] Thomas Ingram, Sandra Storm, Linda Kloss, Tanja Mehling, Sven Jakobtorweihen, and Irina Smirnova. "PRediction of micelle/water and liposome/water partition coefficients based on molecular dynamics simulations, COSMO-RS, and COSMOmic". In: *Langmuir* 29.11 (2013), pp. 3527–3537.

[102] F. Gittes and F. C. MacKintosh. "Dynamic shear modulus of a semiflexible polymer network". In: *Phys. Rev. E* 58 (2 1998), R1241–R1244.

[103] Matteo Pasquali, V. Shankar, and David C. Morse. "Viscoelasticity of dilute solutions of semiflexible polymers". In: *Phys. Rev. E* 64 (2 2001), p. 020802.

[104] Mohammad Hadi Nafar Sefiddashti, Brian J Edwards, and Bamin Khomami. "Elucidating the molecular rheology of entangled polymeric fluids via comparison of atomistic simulations and model predictions". In: *Macromolecules* 52.21 (2019), pp. 8124–8143.

[105] DJ Read, K Jagannathan, SK Sukumaran, and D Auhl. “A full-chain constitutive model for bidisperse blends of linear polymers”. In: *Journal of Rheology* 56.4 (2012), pp. 823–873.

A Discussion on Reversible Scission vs Shuffling

The full-chain population balance equations for reversible scission with reptation were first written down by Peterson and Cates [39] as an exact ensemble-averaged description of the process described in stochastic form by Cates in 1987 [15]. We find it useful to think of the equations as a "population balance" model, since they follow the basic structure of a population balance equation, tracking rearrangements of surviving tube segments in accordance with the reaction kinetics defined by reversible scission. Other readers may find it useful to think of the ordinary reptation equation (cf. equation 1), as a Smoluchowski equation for the distribution of surviving tube segments along a chain; from this perspective, our full-chain population balance equations are simply the Smoluchowski equation for reptation, but extended to include reorganization by reversible scission.

Given that our population balance model captures the same rearrangements as the (previously solved) Pointer model, this Appendix is not concerned with finding accurate solutions to the full equations. Instead, the focus will be pedagocial, seeking to explain the full equations (and their simplification) term-by-term. For a more complete discussion (including equations for out-of-equilibrium $n(L)$, end-attack, and other relaxation processes beyond reptation) we refer the reader to [39].

For a collection of chains reacting by reversible scission, the distribution of surviving tube segments $P(t, s, L)$ in a collection of chains with length L can change through five different processes:

1. Reptation - the endmost surviving segments of a tube are erased through curvilinear diffusion
2. Reaction 1 - chains of length L break into shorter fragments. All contour positions have an equal probability of breaking, so the overall rate of breaking increases with chain length.
3. Reaction 2 - chains of length L join together with another chain to become longer. All end segments are assumed to be equally reactive.
4. Reaction 3 - chains of length $L' > L$ break in a way that generates a new chain of length L (i.e. at contour position $s = L$ or $s = L' - L$)
5. Reaction 4 - Two chains shorter than L combine together to generate a new chain of length L

For the reaction processes (1) - (4) we introduce a pair of conservation rules: (a) when two chains combine, the product chain preserves the surviving tube segments of the reagent chains,

and (b) when a chain is broken, the fragment chains preserve the surviving tube segments of the parent chain. These concepts are demonstrated graphically in Figure 12 and are discussed with more precision in [39].

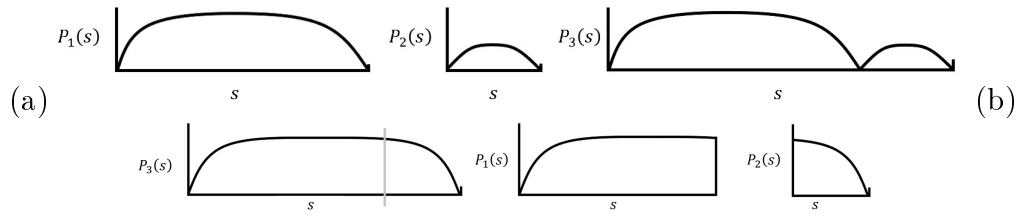

Figure 12: Schematic representation of how surviving tube segments are distributed during (a) recombination and (b) scission. For a more complete discussion, we refer the reader to our prior work.

All these enumerated processes are represented in equation 25, where they appear in the order as listed. Equation 25 assumes that the length distribution remains at equilibrium, $n(t, L) \sim e^{-L/\bar{L}}$, or else there would be additional terms and accompanying population balance equation for the number density distribution function $n(t, L)$.

$$\frac{\partial}{\partial t}P(t,s,L) = M_0\frac{1}{L}\frac{\partial^2 P}{\partial s^2} + \frac{1}{\tau_B}\Bigg[\overbrace{-\frac{L}{\bar{L}}P(t,s,L)}^{\text{loss by breaking}} - \overbrace{2P(t,s,L)}^{\text{loss by breaking}} +$$

$$\overbrace{e^{L/\bar{L}}\frac{1}{\bar{L}}\int_L^\infty dL' e^{-L'/\bar{L}}(P(t,s,L') + P(t,L'-s,L'))}^{\text{production by scission}} +$$

$$\overbrace{\frac{1}{\bar{L}}\int_0^L dL' \begin{cases} P(t,s,L') & \text{if } s < L' \\ P(t,s-L',L-L') & \text{if } s \geq L' \end{cases}}^{\text{production by recombination}}\Bigg] \tag{25}$$

Because reptation and reversible scission are linear operations on the tube survival probability distribution $P(t, s, L)$, the principle of linear superposition applies and the ensemble averaging implied by the equations is exact.

The "production by scission" term in equation 25 employs a "reflection" ($s \to L' - s$) of the tube survival probability distribution inside the argument of the integral. By linear superposition, this reflection is not strictly necessary but is permitted since chains have no natural head or tail. Implementing reflections in this way enforces a symmetry in the resulting solution $P(t, s, L) = P(t, L - s, L)$, which will be helpful when the equations are solved numerically. No additional reflection is needed for the "production by recombination term" since all possible orderings of the

(symmetric) parent chains are already considered (and equally weighted) inside the argument of the integral.

To interpret (or apply) equation 25, the main challenge lies with the integral expressions of the production terms. The simplifying approximations that we introduce in this Appendix section are primarily pedagogical; they are not intended to be realistic, but we believe they are helpful for understanding the physical meaning of the full equations and the relationship between reversible scission and shuffling.

Inside of these integrals, we differentiate between (1) freshly broken chain ends and (2) previously relaxed chain ends. Every time a WLM breaks apart, it produces two freshly broken ends (one on each product chain) and two previously relaxed chain ends. Every time two WLMs combine, two previously relaxed end segments are moved to the chain interior and two previously relaxed ends persist as they were. Stress relaxation is accelerated by the formation of freshly formed ends and rearrangements of previously relaxed ends are less important by comparison.

Our approximation scheme will account for this differentiation as follows: when a chain of length L is produced, (1) freshly broken ends are assumed to have surviving tube segments uniformly and randomly distributed, with mean survival probability $\bar{P}$ and (2) previously relaxed ends are assumed to look similar to the typical end segment in the current population of chains with length L. These assumptions preserve the essential distinction between freshly broken and previously relaxed chain ends.

With these approximations in place, the "production by recombination" term becomes:

$$\frac{1}{\bar{\bar{L}}}\int_0^L dL' \begin{cases} P(t,s,L') & \text{if } s < L' \\ P(t,s-L',L-L') & \text{if } s \geq L' \end{cases} \approx \frac{1}{\bar{\bar{L}}}\int_0^L dL' P(t,s,L) = \frac{L}{\bar{\bar{L}}} P(t,s,L) \tag{26}$$

For the "production by scission" term, we reorganize the reflections (each chain containing one relaxed end and one unrelaxed end) as a superposition of one chain with no relaxed ends and one chain with two relaxed ends. Combining these simplifying approximations, we write:

$$e^{L/\bar{\bar{L}}}\frac{1}{\bar{\bar{L}}}\int_L^\infty dL' e^{-L'/\bar{\bar{L}}}(P(t,s,L')+P(t,L'-s,L')) \approx e^{L/\bar{\bar{L}}}\frac{1}{\bar{\bar{L}}}\int_L^\infty dL' e^{-L'/\bar{\bar{L}}}(P(t,s,L)+\bar{P}(t)) = P(t,s,L)+\bar{P}(t) \tag{27}$$

Combining equation 25 with the simplifying approximations of equations 26 and 27, we get:

$$\frac{\partial}{\partial t}P(t,s,L) = M_0\frac{1}{L}\frac{\partial^2 P}{\partial s^2} + \frac{1}{\tau_B}\Bigg[-\frac{L}{\bar{\bar{L}}}P(t,s,L) - 2P(t,s,L) + \frac{L}{\bar{\bar{L}}}P(t,s,L) + P(t,s,L) + \bar{P}(t)\Bigg] \tag{28}$$

After cancelling terms, this becomes:

$$\frac{\partial}{\partial t}P(t,s,L) = M_0\frac{1}{L}\frac{\partial^2 P}{\partial s^2} + \frac{1}{\tau_B}\left[\bar{P}(t) - P(t,s,L)\right] \tag{29}$$

which is the shuffling model featured in the main text. This is another way of arguing in favor of a constant breaking time as the most reasonable choice for a shuffling model of the full reversible scission rearrangment pathway.

B Extended Discussion of Poisson Renewal

The original Poisson renewal model is attributed to a different sequence rearrangement pathway than the shuffling pathway represented by equation 13. In the main text we have chosen to focus on the shuffling rearrangement pathway for two reasons: (1) the shuffling approximation of Poisson renewal is simpler, and (2) we translated the rearrangement process originally attributed to Poisson renewal into equations for $n(t,L)$ and $P(t,s,L)$ (cf. equations 30 and 33) but found that the bulk rheology predictions are not consistent with equation 14 when τ_B is constant.

The cause of such a disparity is not clear to us - it could be caused by a typo in the original publication or an inaccuracy in the explanation or interpretation of the Poisson renewal process. However it is our view that the main result of the Poisson renewal model, namely equation 14, is more important than the details of its assumed artificial sequence rearrangement pathway. We feel that the shuffling model with length-dependent $\tau_\mathrm{B}(L)$ preserves both the spirit of the original model and its main result, and any disparity at the level of sequence rearrangements is curious but ultimately does not demand careful scrutiny at this point.

The goal of this section is to review the stated mechanism of the original Poisson renewal model and translate it into an equation for the tube survival probability $P(t,s,L)$. In the original Poisson renewal model, "renewal" events cause chains to (1) change length and (2) re-initialize all stress relaxation processes. The length of the renewed chain is drawn from the equilibrium distribution, $n(L) \sim \exp(-L/\bar{L})$, and its surviving tube segments are randomly redistributed to re-initialize all stress relaxation processes. Following these assumptions, the number density distribution evolves as:

$$\frac{\partial}{\partial t}n(t,L) = -\frac{1}{\tau_\mathrm{B}(L)}n(t,L) + e^{-L/\bar{L}}\frac{1}{\bar{L}}\left\langle\frac{1}{\tau_\mathrm{B}}n\right\rangle \tag{30}$$

$$n(t=0,L) = n_0\exp(-L/\bar{L}) \tag{31}$$

$$\left\langle\frac{1}{\tau_\mathrm{B}}n\right\rangle = \int_0^\infty dL'\frac{1}{\tau_\mathrm{B}(L')}n(t,L') \tag{32}$$

The "production" term in equation 30 calculates the total rate of renewal events and then

redistributes those renewed chains in accordance with a defined exponential molecular weight distribution.

Next, a balance equation on surviving tube segments gives:

$$\frac{\partial}{\partial t}(n(t,L)P(t,s,L)) = n(t,L)\frac{M_0}{L}\frac{\partial^2 P}{\partial s^2} - \frac{1}{\tau_{\mathrm{B}}(L)}n(t,L)P(t,s,L) + e^{-L/\bar{L}}\frac{1}{\bar{L}}\left\langle \frac{1}{\tau_{\mathrm{B}}}nP \right\rangle \tag{33}$$

$$\left\langle \frac{1}{\tau_{\mathrm{B}}}nP \right\rangle = \int_0^\infty dL' \frac{1}{\tau_{\mathrm{B}}(L')}n(t,L')\frac{1}{L'}\int_0^{L'} ds' P(t,s',L') \tag{34}$$

The production term in equation 33 follows the same kinetics as the addition of new chains in equation 30, integrating over the entire length distribution to sample every renewal event. Every time a chain of length L' undergoes a renewal event leading to the formation of a chain with length L, tube survival probability in the renewed chain is uniform across all contour positions and equal to the mean tube survival probability prior to the renewal event. Equations 30 and 33 exactly reproduce the original Poisson renewal assumptions, but they do not reproduce the bulk rheology of equation 14. This is difficult to prove for a general case, but for the specific case of a constant breaking time the bulk rheology implied by equations 30 and 33 leads to a slightly different definition of $\langle \eta_0/\tau_{\mathrm{B}} \rangle$, differing only by a factor of z inside the argument of the integral:

$$\langle \eta_0/\tau_{\mathrm{B}} \rangle = \int_0^\infty dz e^{-z}\frac{1}{\tau_{\mathrm{B}}}\left[\sum_{p,\mathrm{odd}}^{\infty}\frac{1}{p^2}[1/\tau_{\mathrm{B}} + i\omega + p^2/\bar{\tau}_{\mathrm{rep}}/z^3]^{-1}\right] \tag{35}$$

C Expanded Summary of Models

This Appendix summarizes a selection of linear rheology models for WLMs, comparing their strengths, weaknesses, and relationships to predecessor models. These notes relay our best current understanding and do not necessarily represent a consensus across the field. Since this is not intended to be a comprehensive list, the choice to include or omit specific models should not be viewed as a value judgement on usefulness. The linear rheology models in Table 1 are mainly the models that were featured (or at least mentioned) in the main text.

The Pointer algorithm basically updates the original Cates model to include (1) a more complete library of physics, (2) a more efficient algorithm to simulate the WLM dynamics, and (3) a complementary protocol to interpret micelle parameters by fitting to rheological measurements. While there have been known issues with prolonged iterations and occasional failure in converging towards a quantitative fit for experimental data, we believe this is mainly due to challenges with the overall nonlinear optimization and fitting process rather than the physics of the model itself. The precise cause of these issues can depend on the initial estimate for model parameters, the noise of experiment data, and the number of iterations allowed for the fitting. A recent work [53]

Linear Rheology Models	Type	Rearrangments	Notes
Cates Original [15]	Stochastic	RS + EA	Method is intuitive but slow compared to Pointer
Lequeux PBE [59]	Continuum	RS	Restricted to single-mode relaxation processes
Poisson Renewal [16]	Continuum	RS + EA (nominal)	Fast and efficient for fitting. Includes corrections for CLF.
Poisson "common pool"	Continuum	RS + EA (nominal)	Pedagogical, not recommended for use
Pointer Algorithm [34]	Stochastic	RS + EA + more	Includes all relevant physics in some form. Known issues with OSFT and fitting algorithm
Full-chain PBE [39]	Continuum	RS + EA	Technically sound but (so far) difficult to use
Shuffling [23]	Continuum	Shuffling	Minor improvement on Poisson renewal
Slip Link [61]	Stochastic	RS	Best treatment of CR and CLF Ideal for low entanglement numbers, $Z < 10$

Table 1: This table summarizes comparisons on the capabilities and limitations of the linear rheology models considered in the main text. This list is not intended to be comprehensive, and the notes reflect our best current understanding. The table uses abbreviations RS (reversible scission), EA (end attack), OSFT (one-side Fourier transform), and CLF (contour length fluctuations).

on the fitting algorithm and iteration protocol demonstrates that the aforementioned issues can be addressed with continued attention and software improvements.

The full-chain population balance model by Peterson and Cates [39] is an ensemble-averaged version of the Langevin equations from the original Cates model. The transformation to a continuum model is exact - there are no approximations beyond those used by Cates, in contrast to the earlier population balance attempt by Lequeux [59]. However, the full-chain population balance model equations (cf. Appendix A) are sufficiently cumbersome that they have not been used. As an alternative, two of us developed the "shuffling model" (cf. section 4) as a useful approximation strategy. It was soon discovered that the shuffling model was a variation of (and slight improvement upon) the original Poisson renewal model (c.f section 4). Corrections for contour length fluctuations (CLF) have also been developed in both frameworks, and in this case it seems that the equations prescribed by Poisson renewal cannot be transformed into a differential constitutive equation for comparison with the shuffling model. Shuffling also includes corrections for double reptation and links to nonlinear rheology models [23], and Poisson renewal prescribes corrections for Rouse modes (though these fail for $\tau_{\mathrm{B}} < \tau_e$).

While the main text (and Appendix A) identifies physical grounds to prefer a shuffling approximation over Poisson renewal, it also shows that in practice there is very little distinction between the two and no practical scientific reason to prefer one over the other. On the other hand, the common pool approximation of section 4.4 has neither a physical basis nor a historical status and cannot be recommended for practical use.